The comparison of Zoledronic acid and romosozumab in calvaria Bone regeneration in ovariectomized rat model

Kyungjin Lee

The Graduate School
Yonsei University
Department of Dentistry

The comparison of Zoledronic acid and romosozumab in calvaria Bone regeneration in ovariectomized rat model

A Dissertation Submitted
to the Department of Dentistry
and the Graduate School of Yonsei University
in partial fulfillment of the
requirements for the degree of
Doctor of Philosophy Dental Science

Kyungjin Lee

December 2024

This certifies that the Dissertation of Kyungjin Lee is approved

Thesis Supervisor Wonse Park

Thesis Committee Member Kee-Deog Kim

Thesis Committee Member Nan-Sim Pang

Thesis Committee Member Jieun Jung

Thesis Committee Member Jisun Huh

The Graduate School
Yonsei University
December 2024

감사의 글

박사 졸업까지 많은 시간이 흘렀습니다. 치과의사가 되고자 결심을 했던 그 순간부터, 4 년간의 치의학전문대학원, 연세대학교 통합치의학과에서의 3 년의 수련, 그리고 6 년간의 박사과정을 통해 배움의 길은 길고도 깊음을 경험했습니다. 임상의로서 살아가는 저에게 박사과정은 새로운 도전이었고, 어려웠지만 제가 더욱 발전되고 성숙할 수 있는 시간이었던 것 같습니다.

이 한편의 논문이 완성되기까지 많은 주변분들의 도움이 있었습니다. 끊임없는 열정과 가르침으로 인도해주신 박원서 지도교수님, 통합치의학과의 든든한 기둥이 되시는 김기덕 교수님, 언제나 사랑으로 반겨주시는 정복영 교수님, 임상의로서 배움의 근간이 된 방난심 교수님, 공직의로서 항상 의지하고 있는 정지은 교수님 감사합니다. 치과대학병원 통합치의학과의 교수님들의 가르침으로 지금의 제가 있게 되었습니다. 무한한 감사드립니다.

또한 바쁘신 와중에도 논문 심사를 맡아주시고 많은 조언과 격려를 해주신 허지선 교수님께도 감사드립니다. 실험의 시작부터 마무리까지 작은 것에서부터 어려운 부분까지 세심하게 신경써주신 박경미 박사님께도 감사합니다. 길지 않은 시간이지만, 연구의 부족한 부분을 메워주시고, 도움을 주신 안현나 박사님께도 감사합니다. 용인세브란스병원 식구들에게도 감사와 애정을 전합니다. 바쁜 딸을 대신하여 손주들을 도맡아주시고 계신 부모님께도 항상 죄송하고 감사한 마음입니다. 학위 마무리까지 기다려주신 시부모님께도 감사하고, 항상 건강하시길 기도하겠습니다. 마지막으로 한결같이 옆에서 지지해준 나의 남편 임준규와 박사 과정 중 태어나 어느새 어린이가 된 나의 사랑하는 두 딸, 예은과 채은에게도 애정과 감사의 마음을 전합니다.

2025 년 1 월 6 일

이경진

TABLE OF CONTENTS

LIST OF FIGURES

ABSTRACT

The comparison of zoledronic acid and romosozumab in calvaria bone regeneration in ovariectomized rat model

Kyungjin Lee

Department of Dentistry
The Graduate School, Yonsei University
(Directed by Professor Wonse Park, D.D.S., M.S.D., Ph.D.)

Purpose

This study aims to evaluate the effects of zoledronic acid and romosozumab on bone regeneration in critical-sized calvarial defects in an ovariectomized rat model of osteoporosis. The research specifically investigates the impact of osteoporosis medications that influence bone metabolism in patients undergoing dental implant placement or bone grafting in alveolar bone defect areas, using an animal model.

Material and Methods

Ovariectomized rats were divided into nine groups based on the type of medication and the duration of administration: control (CONT) 1-week group, control (CONT) 2-week group, control (CONT) 4-week group, zoledronic acid (ZA) 1-week group, zoledronic acid (ZA) 2-week group, zoledronic acid (ZA) 4-week group, romosozumab (RM) 1-week group, romosozumab (RM) 2-week group, and romosozumab (RM) 4-week group. The CONT group received no medication, whereas the ZA and RM groups were administered zoledronic acid and romosozumab, respectively, for 1, 2, and 4 weeks.

A 5 mm circular defect was created bilaterally in the calvaria of all experimental animals. Bone grafting was performed on one side, while the other side was left without grafting. To evaluate the systemic effects of the medications, radiological and histological examinations of the tibia were conducted. Radiological, histological, and immunohistochemical analyses were performed on the calvarial defect sites to assess bone regeneration.

Results

In the tibia, the RM 2-week and 4-week groups demonstrated an increase in trabecular thickness, resulting in an overall increase in bone volume fraction. In the grafted calvarial defects, histomorphometric analysis revealed that the RM 4-week group formed significantly more new bone compared to the CONT group, showing a statistically significant difference. However, immunohistochemical analysis showed no statistically significant differences in the expression of RANKL, OPG, or sclerostin among the groups. In the ungrafted calvarial defect sites, radiological and immunohistochemical analyses did not reveal any distinct differences between the medication groups and the CONT group

Conclusions

In the tibia, romosozumab demonstrated a more pronounced effect compared to zoledronic acid, increasing trabecular thickness and overall bone volume. However, in the calvarial defect sites, no significant differences in bone regeneration were observed between zoledronic acid and romosozumab, regardless of whether bone grafting was performed.

These findings are thought to be attributable to anatomical and developmental differences between the tibia and the calvaria, suggesting a variation in their responses to the medications during the early phases of treatment. Further research is warranted to explore the long-term effects of these medications, which may provide critical insights into their impact on bone regeneration in the jaw bone. This study holds value as foundational research into the effects of osteoporosis medications on bone regeneration in the maxillofacial region.

Keywords: zoledronic acid, romosozumab, osteoporosis, critical size defect, bone regeneration

1. Introduction

The World Health Organization (WHO) defines osteoporosis as a systemic skeletal disease characterized by decreased bone mass and microarchitectural deterioration, resulting in increased bone fragility and susceptibility to fractures (1,2). Bone mass is primarily expressed as bone mineral density (BMD), while bone quality encompasses factors such as structure, turnover, mineralization, and microdamage accumulation. Osteoporosis is diagnosed using BMD measurements (3). The most common cause of osteoporosis is postmenopausal estrogen deficiency, which is characterized by an increased bone turnover rate due to elevated bone resorption relative to bone formation (4). Osteoporosis treatments aim to reduce fracture risk at sites such as the hip, wrist, and vertebrae by increasing BMD and decreasing bone turnover (4-6).

Osteoporosis medications are broadly classified into anti-resorptive agents and anabolic agents based on their mechanisms of action. Representative anti-resorptive agents include bisphosphonates and denosumab, while anabolic agents include parathyroid hormone and romosozumab (3).

Bisphosphonates are anti-resorptive agents used for the prevention and treatment of osteoporosis. They bind to the mineral matrix of bone and are absorbed by osteoclasts, inhibiting osteoclastic activity, reducing bone turnover, and consequently increasing bone mass, mineralization, and BMD. This leads to enhanced bone strength and reduced fracture risk (7,8). Based on their structure, bisphosphonates can be categorized into non-nitrogen-containing and nitrogen-containing compounds, with differences in their mechanisms of action on osteoclasts. Nitrogen-containing bisphosphonates, such as zoledronic acid, target osteoclasts by interfering with the cholesterol biosynthesis pathway within the cells. This mechanism allows the drug to achieve therapeutic effects even at low doses, making it effective for the treatment of conditions characterized by rapid bone

destruction, such as postmenopausal osteoporosis, Paget's disease, and bone metastases associated with malignant tumors (9,10).

Romosozumab is a humanized antisclerostin monoclonal antibody (11). Sclerostin, a key inhibitor of the canonical Wnt signaling pathway, binds to LRP-5/6 and prevents Wnt proteins from interacting with Frizzled receptors and LRP co-receptors, thereby suppressing the Wnt signaling pathway (12). This suppression leads to reduced osteoblast differentiation and function, ultimately decreasing bone formation (11). Additionally, sclerostin indirectly stimulates bone resorption by influencing the RANKL/OPG system. Activation of the Wnt signaling pathway promotes the expression of osteoprotegerin (OPG), which inhibits the action of RANK ligand (RANKL). Sclerostin reduces OPG levels and enhances RANKL activity, promoting bone resorption. Romosozumab, by inhibiting sclerostin, reduces the RANKL/OPG ratio, thereby exerting an anti-resorptive effect (13).

There are conflicting findings regarding the effects of bisphosphonates on healing following dental surgical treatments. Some studies have reported that bisphosphonate administration negatively impacts bone metabolism, leading to delays in bone repair and formation at tooth extraction sites (14). On the other hand, other studies suggest that short-term alendronate therapy does not affect bone formation after tooth extraction and may improve bone filling in the extraction socket (15). In terms of implant osseointegration, some reports indicate that bisphosphonates increase the bone mineral density around the implant (16), and enhance implant osseointegration (17). However, other studies suggest that bisphosphonates may have a negative impact on the integration between bone and implant threads (18).

Although the clinical use of sclerostin antibody (Scl-Ab) has been shorter compared to bisphosphonates, resulting in relatively fewer studies, previous animal experiments have demonstrated the anabolic effects of Scl-Ab in areas such as the tibia, femur, and vertebrae, as well

as its impact on fracture healing models (19–21). Animal studies have shown that systemic Scl-Ab administration enhances osseointegration and bone regeneration around dental implants (22). Additionally, research has indicated that Scl-Ab helps restore alveolar bone mass following experimental periodontitis (23,24).

Clinically, patients on osteoporosis medications may require oral reconstruction through dental implant placement. When placing dental implants in cases of atrophic alveolar ridges or bone defects, guided bone regeneration (GBR) using barrier membranes has become a standard procedure. Animal studies have reported the effectiveness of graft materials or GBR in healing bone defects using critical size defect models (25). However, there are few comparative studies examining the impact of medications that affect bone metabolism on bone regeneration in critical size defect models. This study aims to experimentally induce osteoporosis and compare the effects of bisphosphonates and romosozumab, which have different mechanisms of action, on the healing of calvarial bone defects, with or without the use of bone graft materials.

2. Materials and methods

2.1. Animals

A total of 103 twelve-week-old Sprague-Dawley rats were used and randomly divided into 9 groups. All groups of rats were ovariectomized, and excluding those that died during the experiment, results were obtained from a total of 95 rats. The body weight of the animals was measured weekly.

Animals were housed under standard laboratory conditions (temperature 20°C ± 5°C, humidity 50% ± 10%, lighting cycle, 12 h light/12 h dark). All animals have free access to water and were fed a standard laboratory pellet diet. The animal selection, management, surgical protocol, and preparation followed routine protocol approved by the Institutional Animal Care and Use Committee of Yonsei Medical Center, Seoul, Korea.

2.2. Experimental design

Bilateral ovariectomy (OVX) was performed under general anesthesia in all animals. After 8 weeks of OVX, calvarial surgery was conducted. A full-thickness flap was elevated to expose the calvaria, and a trephine bur was used to create 5mm circular defects bilaterally, centered along the sagittal suture. Deproteinized bovine bone mineral was used as a bone graft material in the one defected area, which was covered with collagen membranes . The other defect was left ungrafted, with only the membrane covering the defect. The Control group received no medication, while the ZA group (Zometa ready®, Novartis, Basel, Switzerland; 40μg/kg/day, IV once a week for 1, 2, and 4 weeks) and the RM group (Evenity®, Amgen, Thousand Oaks, CA; 25mg/kg/day, SQ twice a week for 1, 2, and 4 weeks) were treated with their respective medications. The animals were subsequently sacrificed according to the study protocol. (Figure 1)

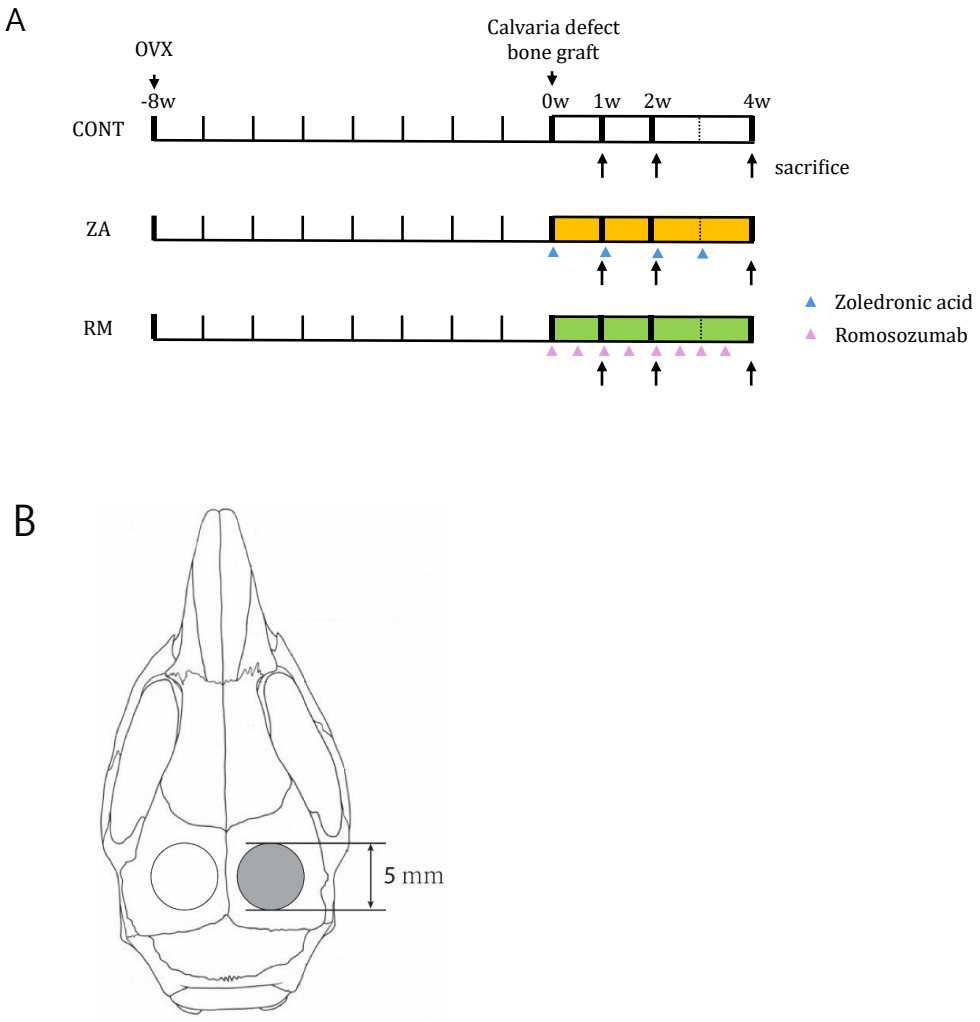

Figure 1. Experimental design. (A) Time table, (B) Calvaria defect : non-graft left side / graft right side. ZA=Zoledronic acid group, RM=Romosozumab group

2.3. Surgical procedure

Bilateral ovariectomy (OVX) on all animals was performed under general anesthesia by intraperitoneal injection of combined Zoletil® (tiletamine and zolazepam, 50 mg/ml, 0.6 ml/kg body mass; Virbac lab. Carros, France) and Rompun® (zylazine, 23.32 mg/ml, 0.4ml/kg body mass; Bayer, Leverkusen, Germany). After surgery, meloxicam (1 mg/kg, once a day for 5 days; Metacam®, Boehringer Ingelheim, Rhein, Germany) and enfloxacin (10 mg/kg/day, once a day for 5 days, Baytril®, Bayer, Germany) were subcutaneously administered.

After an 8-week development of osteoporosis in the OVX rats, calvaria surgery was operated. In the calvaria surgery, The calvaria bone was exposed, and 5-mm circular defects both right and left side were created using a trephine bur. Deproteinized bovine bone mineral (Bio-Oss®, Geistlich Pharma, Wolhusen, Switzerland) was used as a bone graft materials in the right side defected area and covered with collagen membranes (Bio-gide®, Geistlich Pharma, Wolhusen, Switzerland). The left side underwent no bone grafting and was covered only with a collagen membrane. The flaps were closed with absorbable 4-0 Vicryl® (Vicryl®, Ethicon, Somerville, NJ, US).

2.4. Assessment

2.4.1. Radiographic analysis: micro-computed tomography (micro-CT)

Block sections, including the tibia, calvaria defects, and surrounding tissue, were excised and fixed in formalin for 7 days. All fixed specimens were scanned using micro-computed tomography (SkyScan 1173, SkyScan, Kontich, Belgium) with a pixel size of 7.12 μm (tibia) and 13.88 μm (calvaria) under conditions of 130 kV and 60 μA. The images were reconstructed and analyzed using CTAn software (SkyScan, Aartselaar, Belgium).

To evaluate the systemic effects of the administered drugs, the trabecular bone in the proximal tibia was analyzed. The volume of interest (VOI) was defined as the region extending from 0.7 mm below the growth plate to 3.5 mm distally. (Figure 2).Parameters assessed within the VOI for trabecular bone included the bone volume fraction (BV/TV), trabecular thickness (Tb.Th), trabecular number (Tb.N), and trabecular separation (Tb.Sp)(26).

For the calvaria bone defect, the Volume of Interest(VOI) on the graft side included both the graft material and newly formed bone, confined within a cylinder defined by the defect margins and surrounding bone. On the non-grafted side, all defect areas and newly formed tissues were selected for analysis. (Figure 3) To differentiate between new bone and graft material on the graft side, gray scale thresholds were set as follows:

- Total bone: Gray scale 35–255
- Residual grafted material: Gray scale 54–255
- New bone: Gray scale 35–53

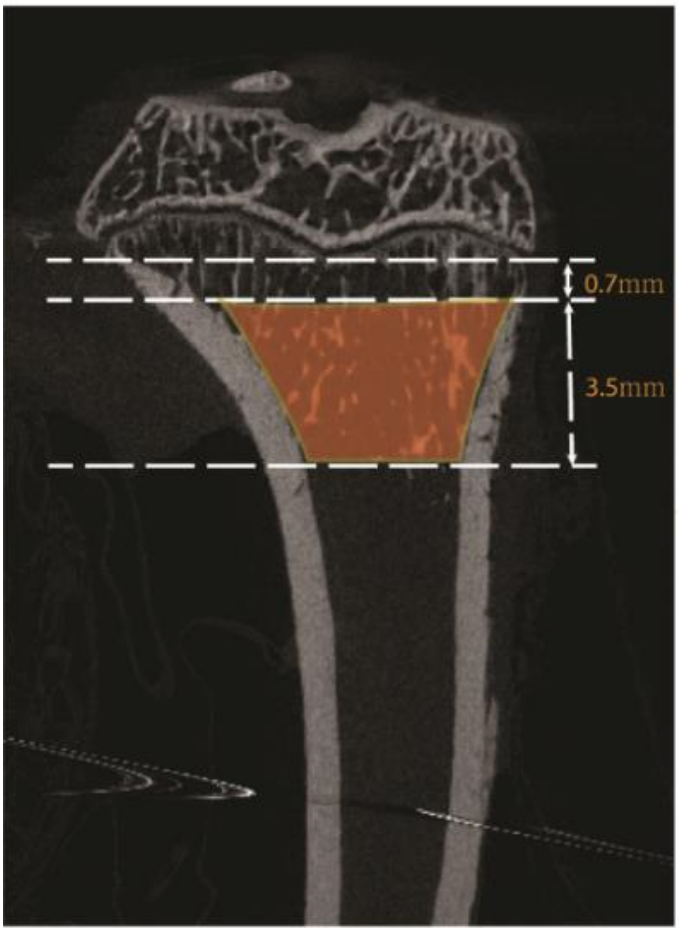

Figure 2. The volume of interest in micro-CT analysis for trabecular bone of tibia

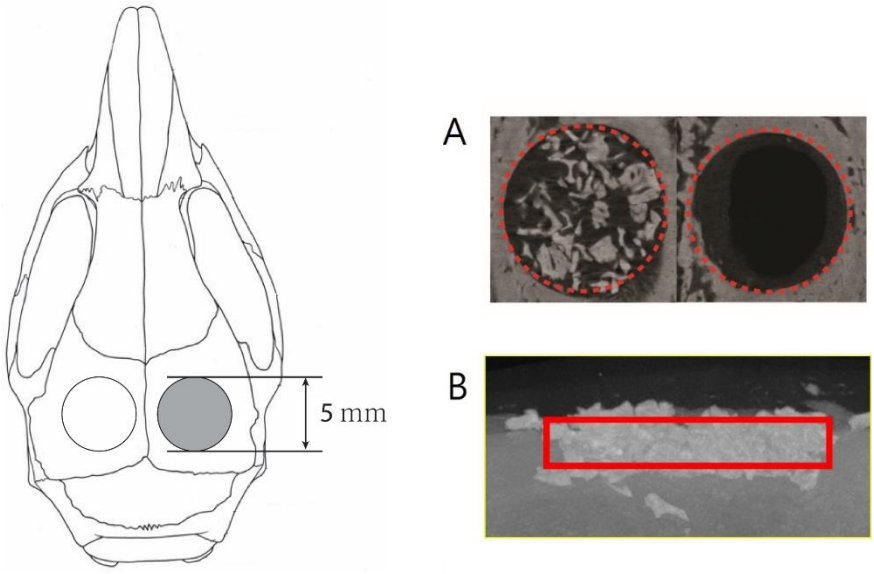

Figure 3. The volume of interest in micro-CT analysis for calvaria defect**.**

2.4.2. Histological analysis

After micro-CT scanning, the block specimens were decalcified with 5% HCl and embedded in paraffin. The blocks were serially sectioned in a 5 μm coronal plane. Hematoxylin and eosin (H&E) staining were done according to the manufacturer's recommendations. The images were observed by light microscope (OLYMPUS BX43, UIS2 optical system, Olympus Corporation, Tokyo, Japan). Histological images are examined a magnification using Slideviewer (3DHISTECH Ltd, Budapest, Hungary).

2.4.3. Histomorphometric analysis

The images were analyzed histomorphometrically by two masked, experienced observers using a PC-based image system (Photoshop, Adobe Systems, San Jose, CA, USA).

In Hematoxylin-Eosin-stained slides, the boundaries of the total augmented area (TAA) were delineated, and new bone and residual material observed in the slides were distinguished using different colors. The following parameters were measured. (Figure 4):

- Total augmented area (TAA, mm^2)
- New bone area (NBA, mm^2) : NBA/TAA = %NBA
- Residual material area (RMA, mm^2) : RMA/TAA = %RMA
- Connective tissue area (CTA, mm^2) : CTA/TAA = %CTA

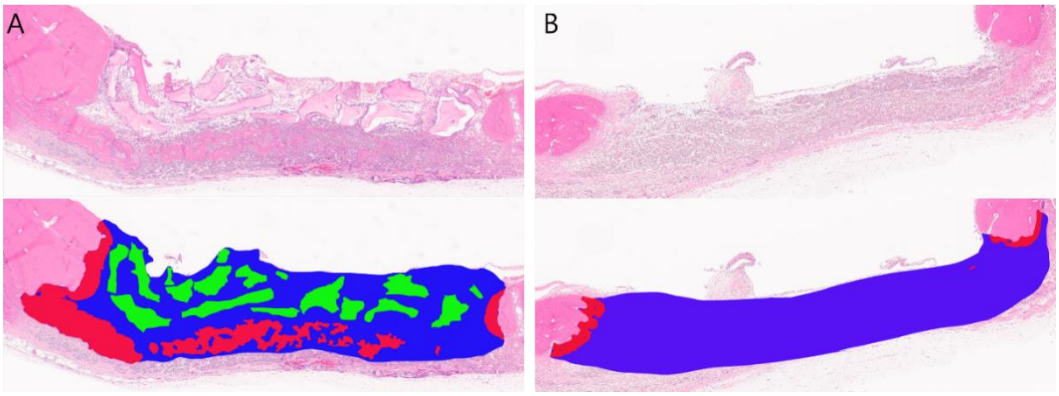

Figure 4. Histomorphometric analysis (A) Graft side (B) Non graft side. (Red indicates new bone, blue represents connective tissue, and green denotes residual material.

2.4.4. Immunohistochemical analysis

From the calvaria bone slides, three samples were randomly selected for immunohistochemical (IHC) analysis. For IHC staining, paraffin blocks were sectioned at a thickness of 4 μm. All staining procedures, from deparaffinization to counterstaining, were performed using an automated Ventana Discovery XT staining instrument (Ventana Medical Systems, Inc., Tucson, AZ, USA).

The following primary antibodies were used: Mouse anti-RANKL monoclonal antibody (1:7000 dilution; sc-377079, Santa Cruz, USA), Rabbit anti-OPG polyclonal antibody (1:500 dilution; ab203061, Abcam, USA), Rabbit anti-sclerostin polyclonal antibody (1:400 dilution; ab85799, Abcam, USA). Secondary antibodies were selected and applied according to the manufacturer's instructions. The sections were visualized using a diaminobenzidine (DAB) coloration kit, followed by counterstaining with hematoxylin.

For the analysis of calvaria bone, three regions (medial, central, and lateral) were randomly selected from both the graft and non-graft sides, using the sagittal suture as the reference point. A 0.2 mm × 0.2 mm region was defined as the region of interest (ROI) for each site (500× magnification). To measure the IHC staining intensity, ImageJ software (version 1.53, National Institutes of Health, USA) with the IHC Profiler plugin was utilized (27). The expression levels were quantified by calculating an H-score (28,29). The H-score was determined by summing the percentage of strongly stained nuclei (3×), moderately stained nuclei (2×), and weakly stained nuclei (1×). The H-scores from the medial, central, and lateral regions were combined to generate a single H-score for each slide. Histological images were examined at ×500 magnification using SlideViewer software (3DHISTECH Ltd, Budapest, Hungary).

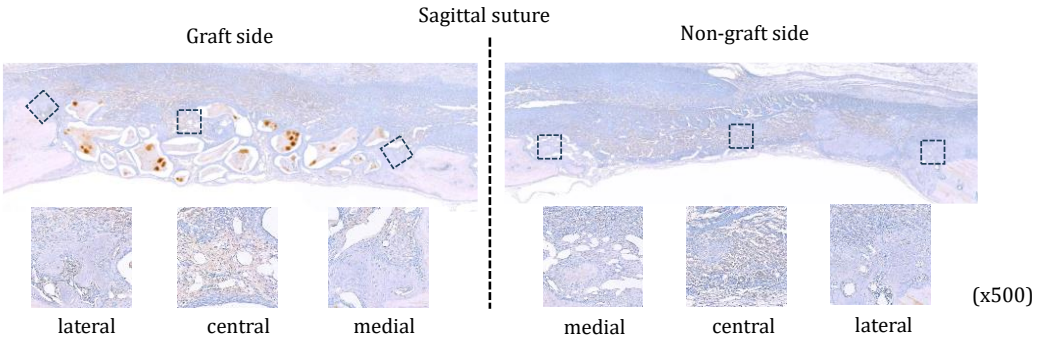

Figure 5. Region of Interest for Immunohistochemical Analysis : The H-score was calculated for the mesial, center, and distal regions, and the scores were summed to determine the H-score for each slide.

2.4.5. Statistical analysis

Statistical analysis was performed using IBM SPSS software (version 27.0, IBM Corp., Armonk, NY, USA).

To account for the sample size, the data were first tested for normality. Since the data did not follow a normal distribution, a nonparametric approach was applied. The Kruskal-Wallis test was used to compare the sizes of the three groups ($p < 0.05$). For post-hoc analysis, the Mann-Whitney test was conducted to evaluate differences between individual groups. The level of significance was adjusted using Bonferroni correction, and the threshold was set at $p < 0.05/3 = 0.017$.

.

3. Results

3.1. Animal body weight

The average body weight of the animals before ovariectomy (OVX) was 263 g, and all individuals showed an increasing trend in body weight until sacrifice after OVX. (Figure 6)

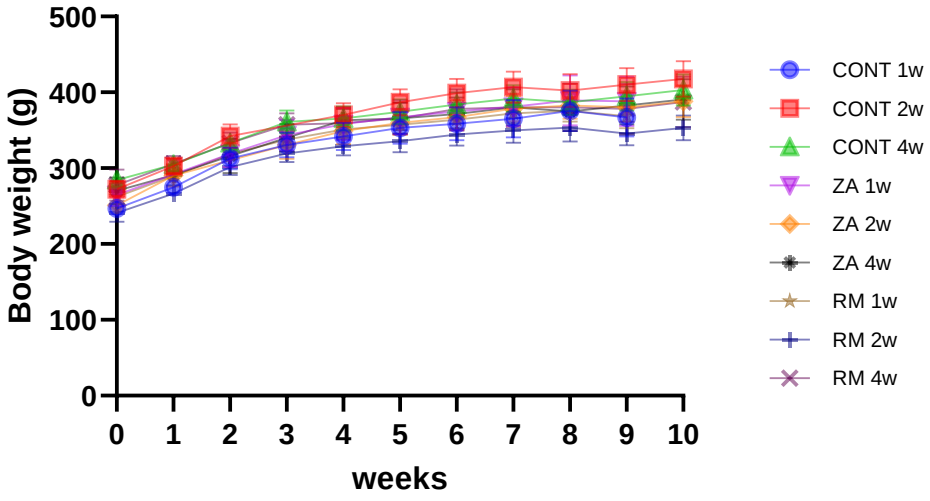

Figure 6. Body weight of animals

3.2. Long bone : tibia

3.2.1. Radiographic analysis: micro-computed tomography (micro-CT)

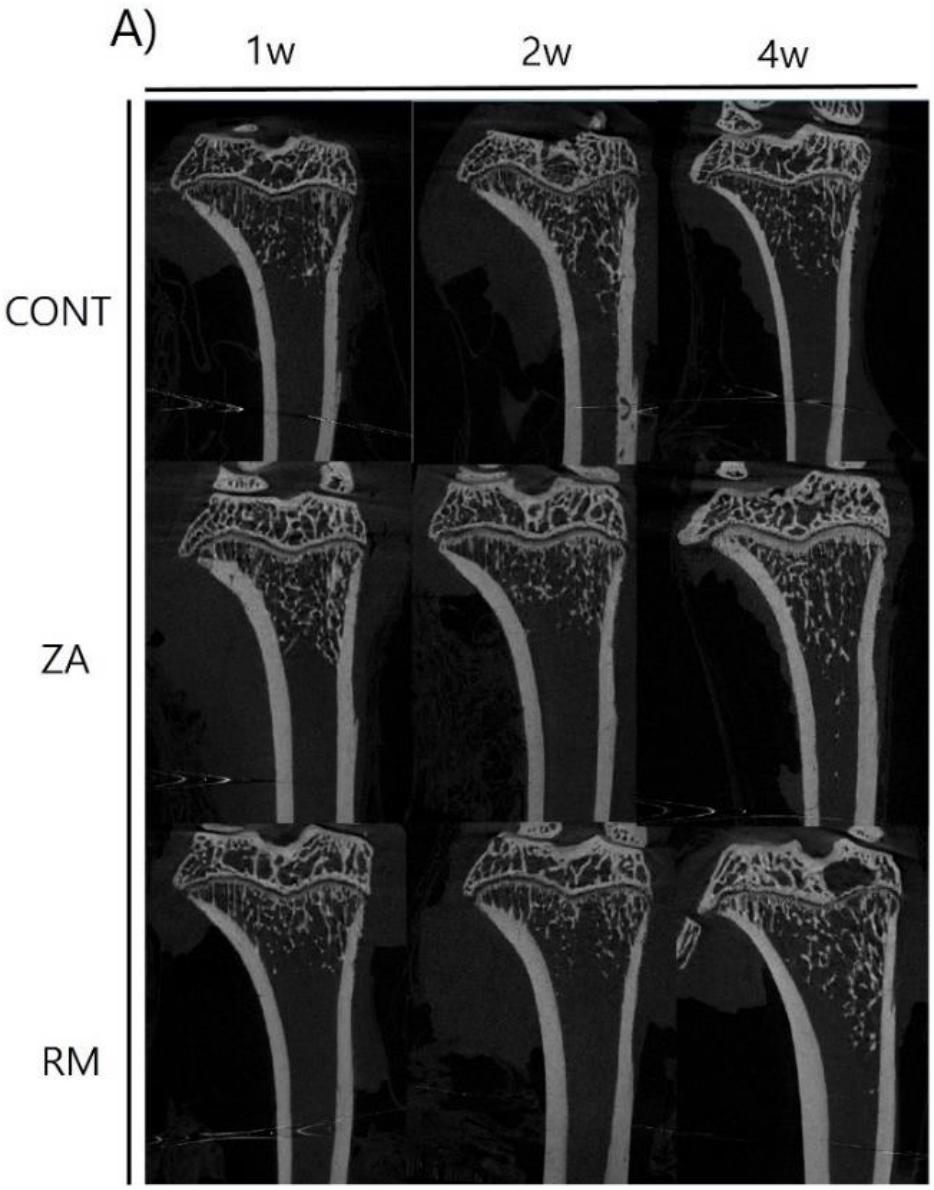

Figure 7 (A). Micro-CT image of tibia : Longitudinal cross-section image.

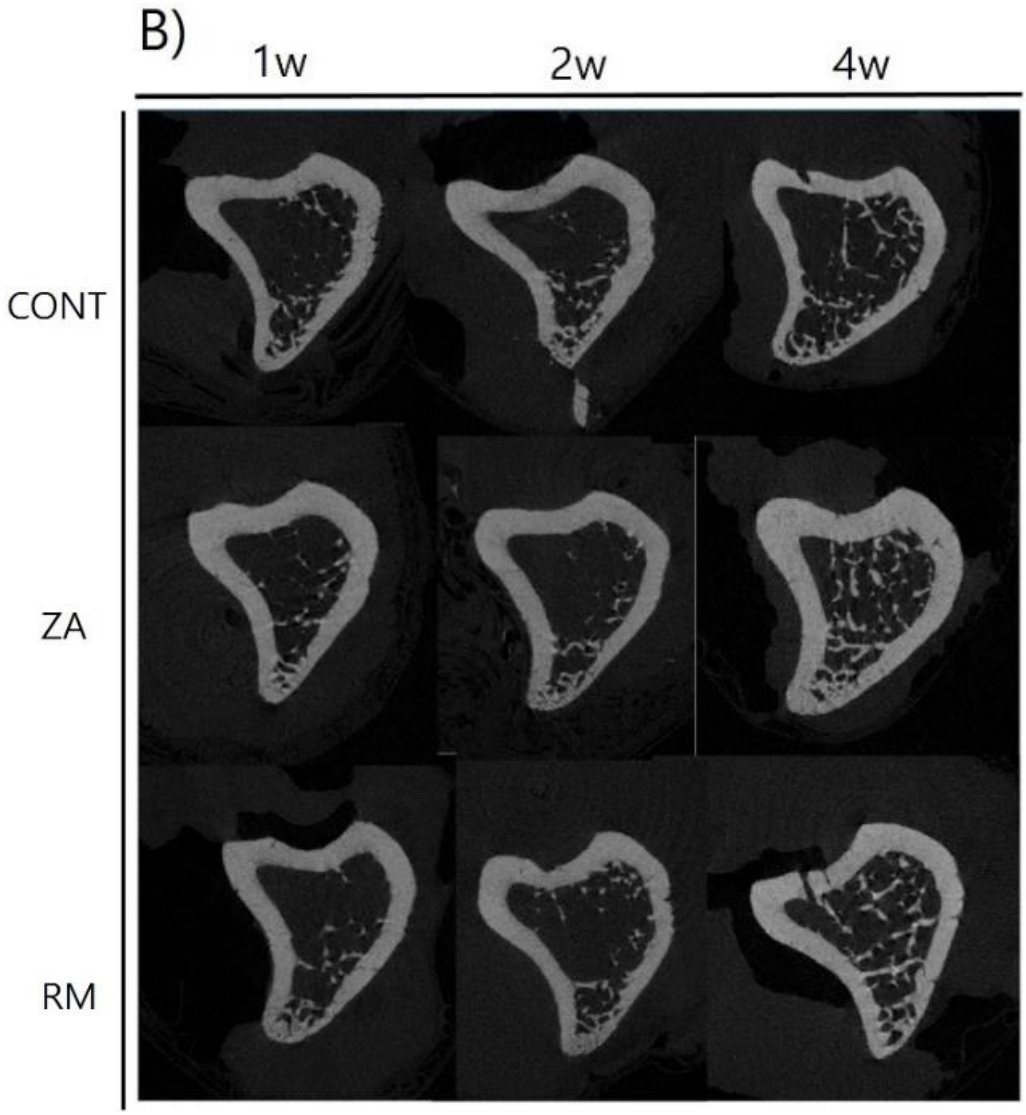

Figure 7 (B) . Micro-CT image of tibia : cross-section image.

As the duration of drug administration increased, the trabecular pattern became more distinct. In particular, the RM-treated group exhibited a pronounced trabecular pattern within the VOI, while the ZA-treated group showed thickening around the growth plate. (Figure 7)

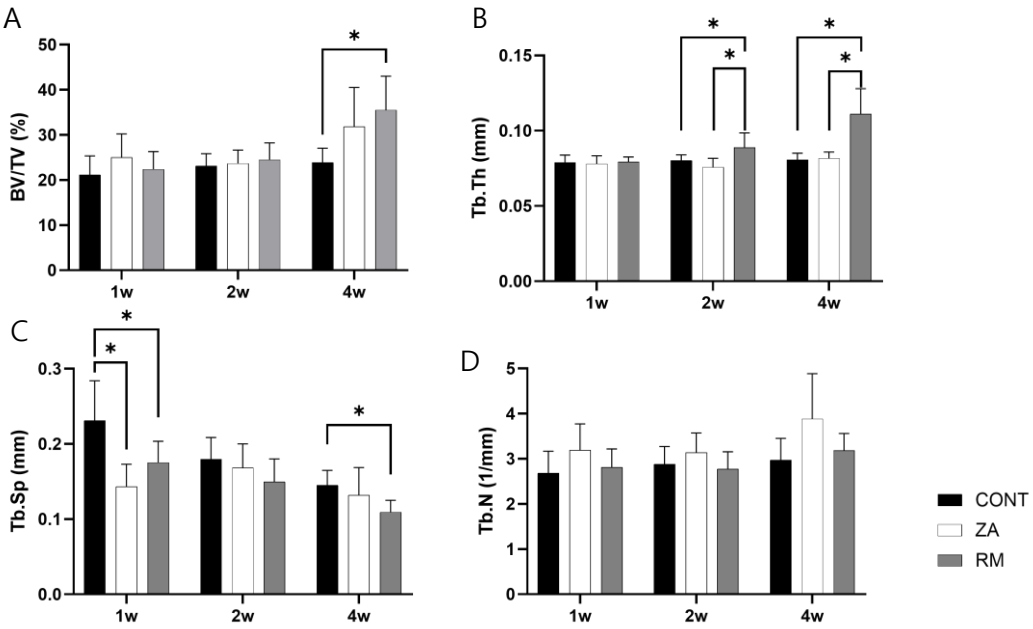

Figure 8. Micro-CT analysis of tibia : (A) Bone volume fraction (BV/TV, %), (B) Trabecular thickness (Tb.Th, mm), (C) Trabecular number (Tb.N, 1/mm), (D) trabecular separation (Tb.Sp, mm). * indicate P<0.017

In the 1-week treatment group, the ZA and RM groups showed a difference in trabecular separation compared to the CONT group. In the 2-week and 4-week treatment groups, the RM group exhibited thicker trabeculae compared to the CONT and ZA groups. Consequently, in the 4-week treatment group, the RM group showed an increased bone volume fraction compared to the other treatment groups. (Figure 8)

3.2.2. Histologic observation

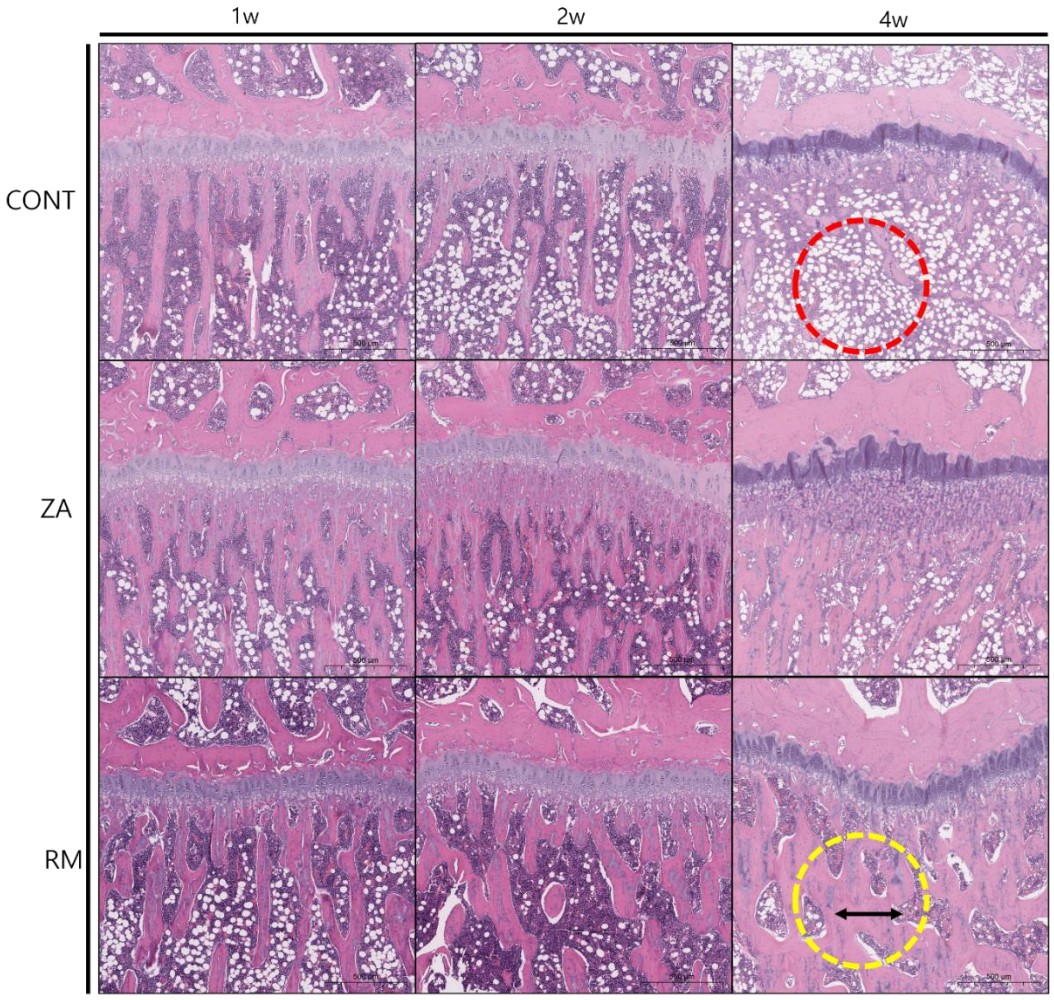

Figure 9. Longitudinal cross-section image of the proximal tibia - Hematoxylin and Eosin staining (100× magnification)

In the CONT group at 4 weeks, compared to the 1-week treatment group, an increase in adipocytes within the trabecular bone was observed, exhibiting characteristics of osteoporosis in long bones (red dashed line). In the RM group, trabecular thickness progressively increased by the 4-week time point (yellow dashed line). (Figure 9)

3.3. Calvaria bone : graft site

3.3.1. Radiographic analysis : micro-computed tomography (micro-CT)

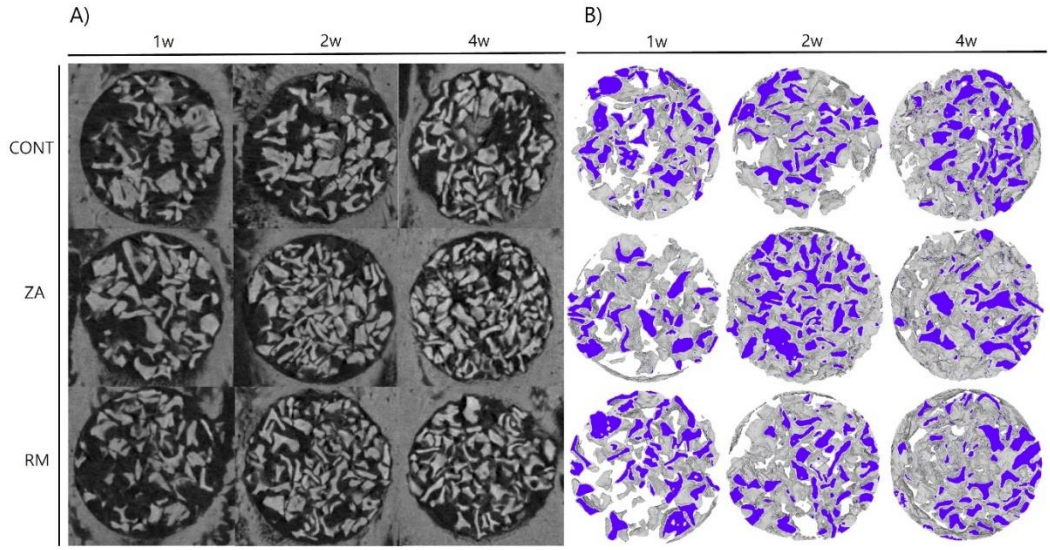

Figure 10. Micro-CT of calvaria bone : graft side (A) micro-CT image. (B) 3D modeling of calvaria bone defect on the graft side. The region of interest (VOI) was segmented based on the defined gray scale: new bone (blue, gray scale: 35-53) and graft material (gray, gray scale: 54-255).

Figure 10 (B) is 3D modeling of the calvaria bone defect VOI. It can be observed that from the 1-week to 4-week time points, the total volume (new bone + residual material) increases.

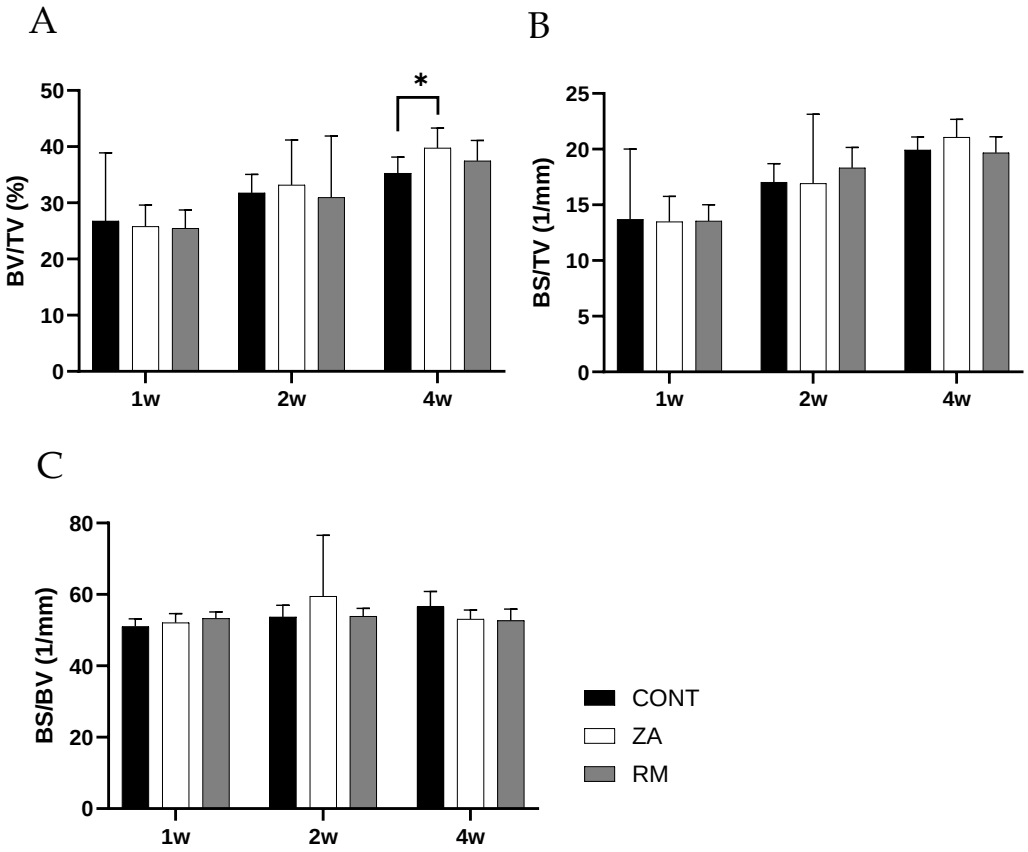

Figure 11. Micro-CT analysis of calvaria graft side: Total bone (gray scale : 35-255) (A) Bone volume fraction (BV/TV, %), (B)Bone surface density (BS/TV,1/mm), (C) Specific bone surface (BS/BV, 1/mm) . * indicate P<0.017

When examining the total bone, which includes both new bone and graft material, it was observed When evaluating the total bone, which includes both new bone and graft material, it was observed that as the medication administration period increased, the bone volume fraction also increased. A significant difference was noted between the CONT and ZA groups at the 4-week mark, with an increase in bone volume fraction, but no further differences were observed beyond that. Similarly, bone surface density showed an increasing trend, but no statistical differences were found. (Figure 11)

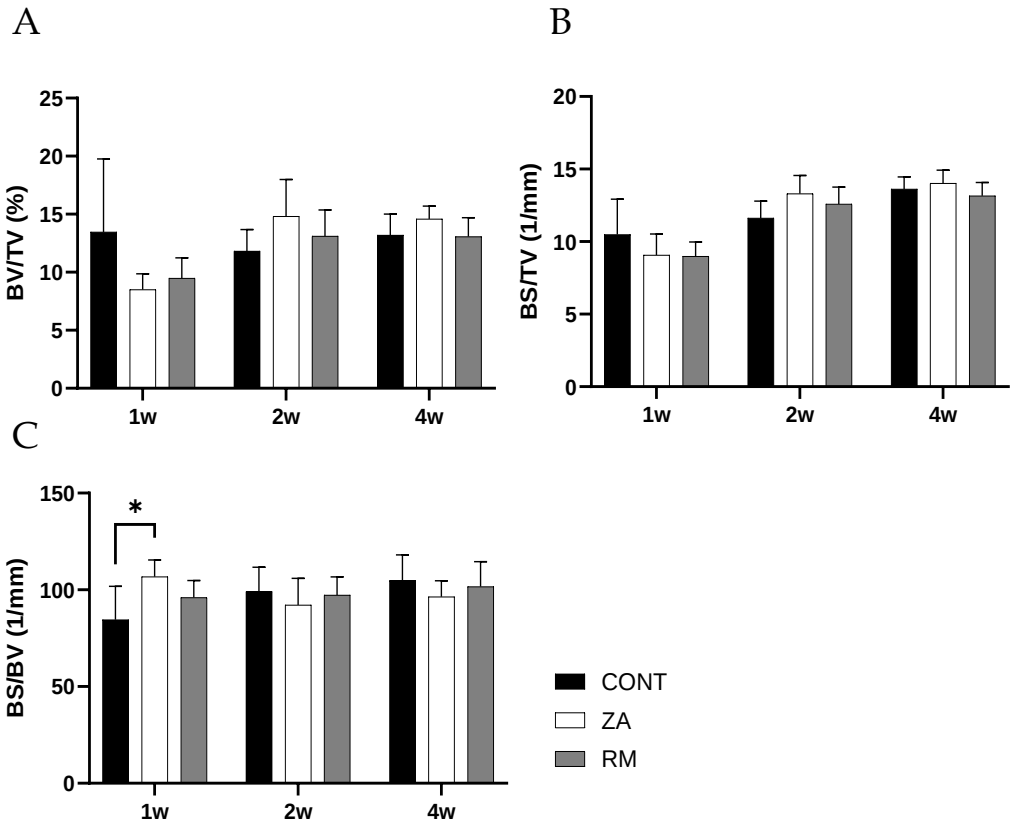

Figure 12. Micro-CT analysis of calvaria graft side : New bone (gray scale : 35-53) (A) Bone volume fraction (BV/TV, %), (B)Bone surface density (BS/TV,1/mm), (C) Specific bone surface (BS/BV, 1/mm)

When measuring only the new bone area (gray scale: 35-53), no significant increase in bone volume fraction was observed, even as the drug administration period increased, and no statistical differences were found. The CONT and ZA groups showed a difference in specific bone surface at the 1-week time point, but no other clear differences were observed. Additionally, no differences between the drugs were found in bone volume fraction or bone surface density. (Figure 12)

3.3.2. Histological observation

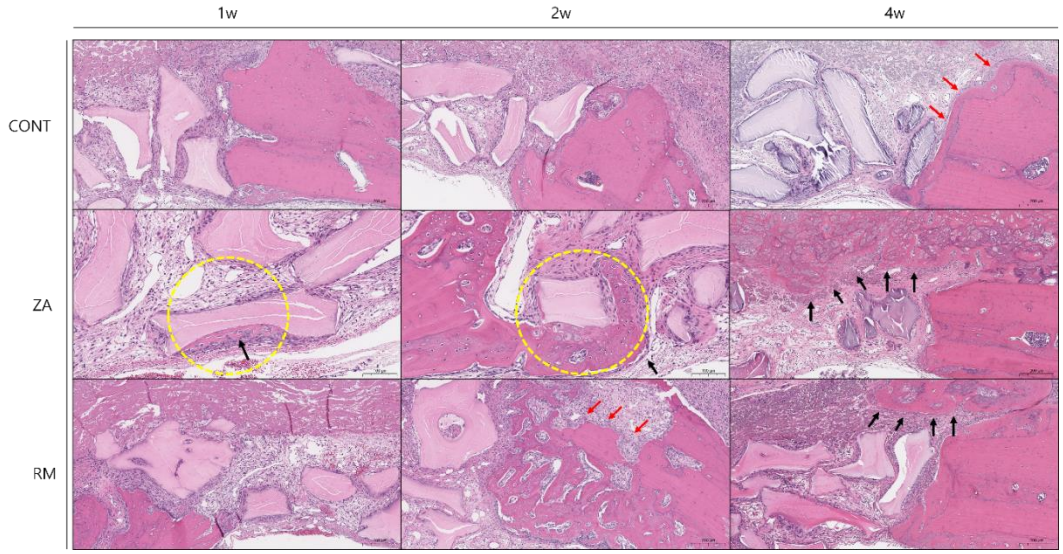

Figure 13. Histological findings in calvaria defect grafted area H&E staining (100x).

At the defect margin, new bone formation is observed along the reversal line (red arrow). New bone forms around the material (yellow dashed line), and new bone formation is also seen both above and below the defect margin (black arrow). (Figure 13)

3.3.3. Histomorphometric analysis

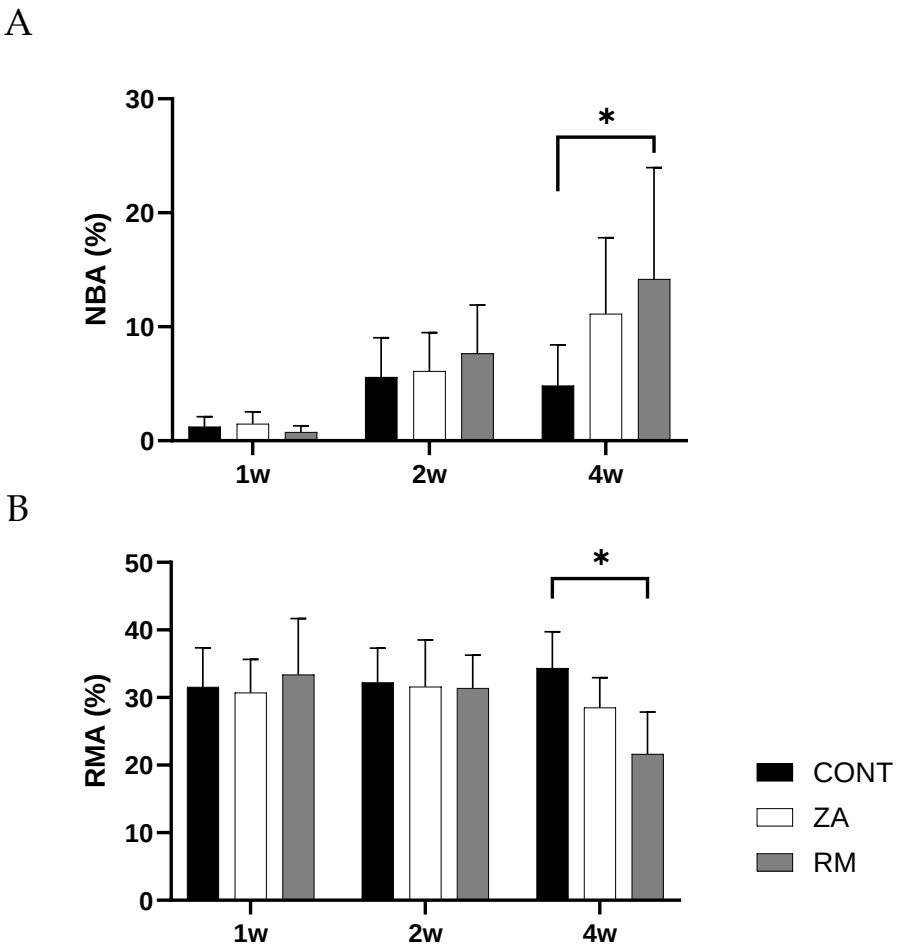

Figure 14. Histomorphometric analysis of calvaria graft side. * indicate p<0.017

Based on histological observations on the graft side, the percentage of new bone area and residual material area were calculated through area measurements. After 4 weeks of drug administration, the RM group showed more new bone formation compared to the control, and as a result, the amount of graft material was reduced. (Figure 14)

3.3.4. Immunohistochemical(IHC) analysis

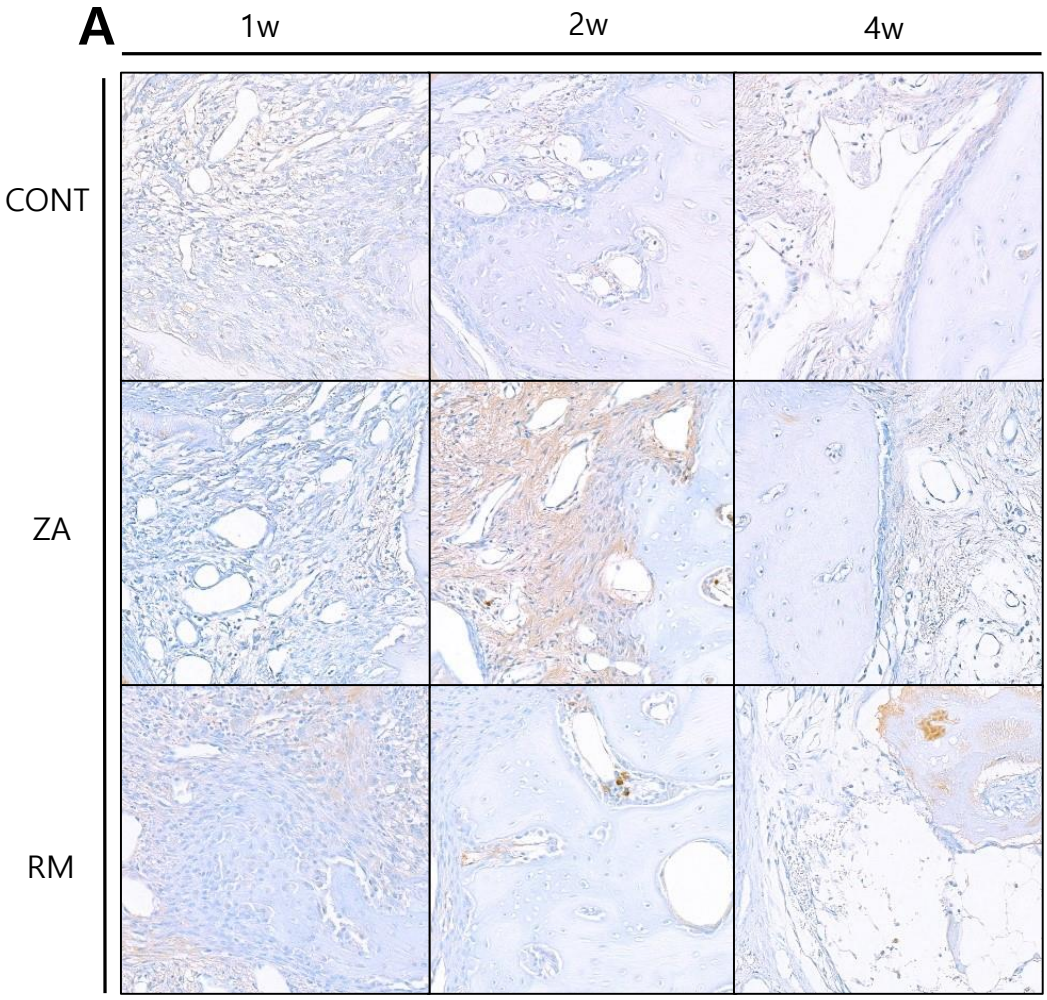

Figure 15. Immunohistochemical analysis of calvaria graft side : RANKL medial side image.

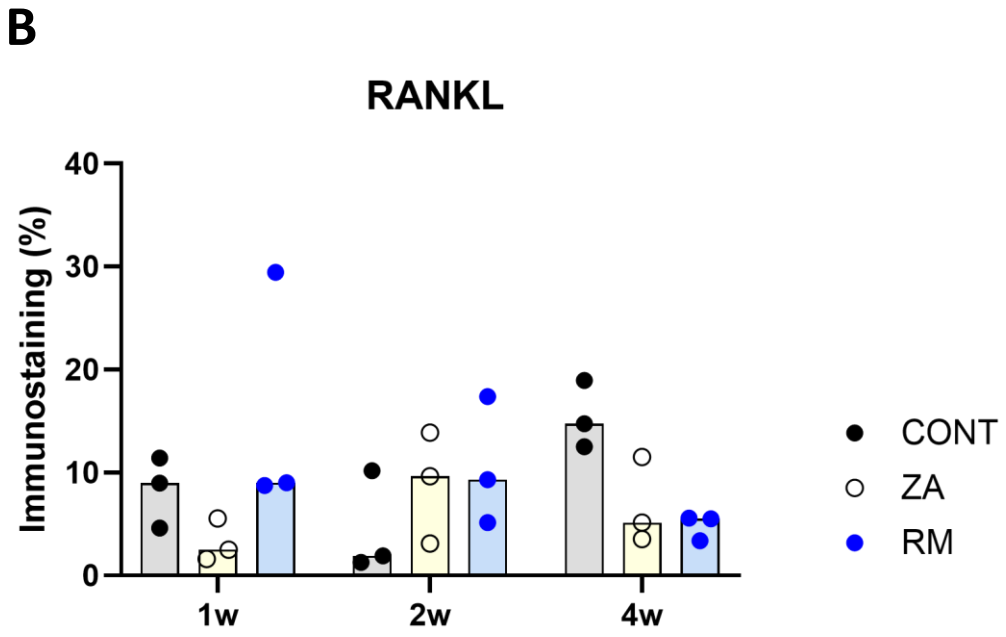

Figure 16. H-score of RANKL on graft side : scatter plat, median with bar

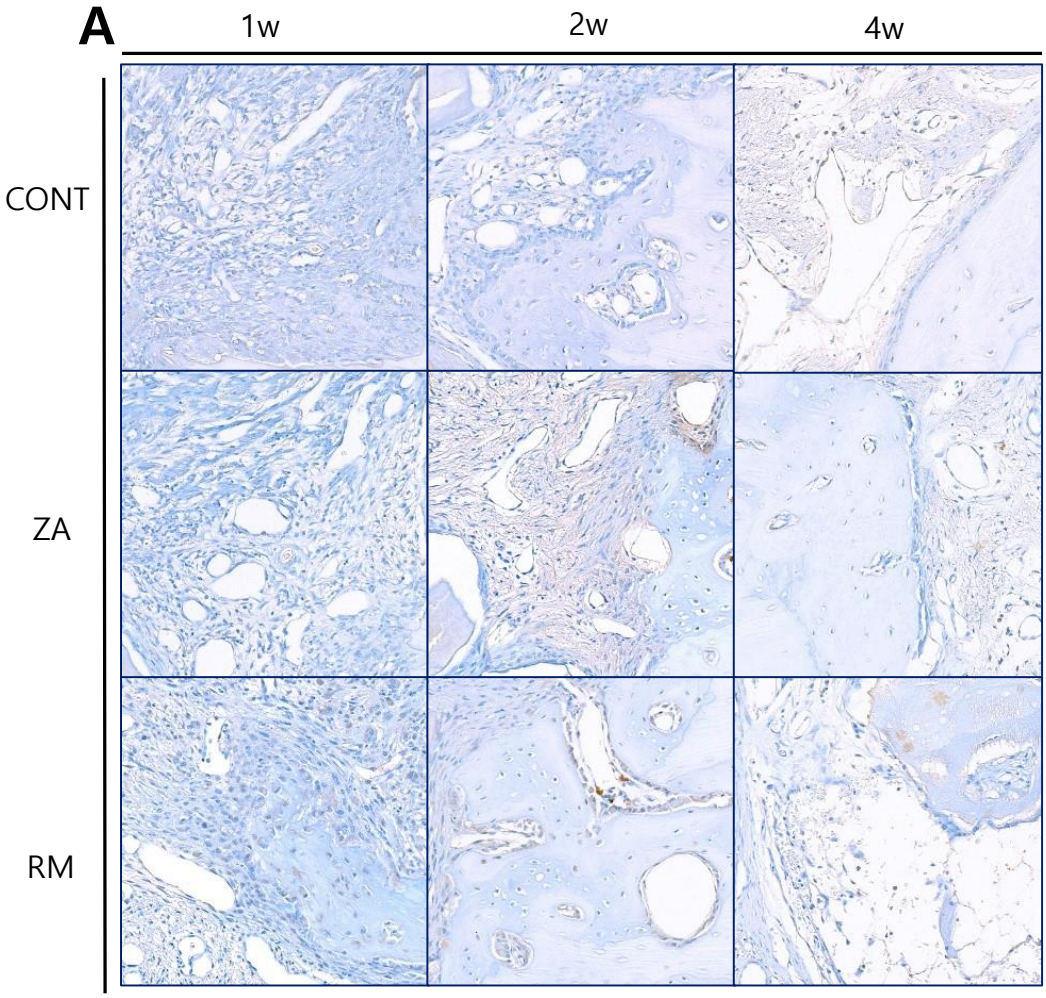

Figure 17. Immunohistochemical analysis of calvaria graft side : OPG medial side image.

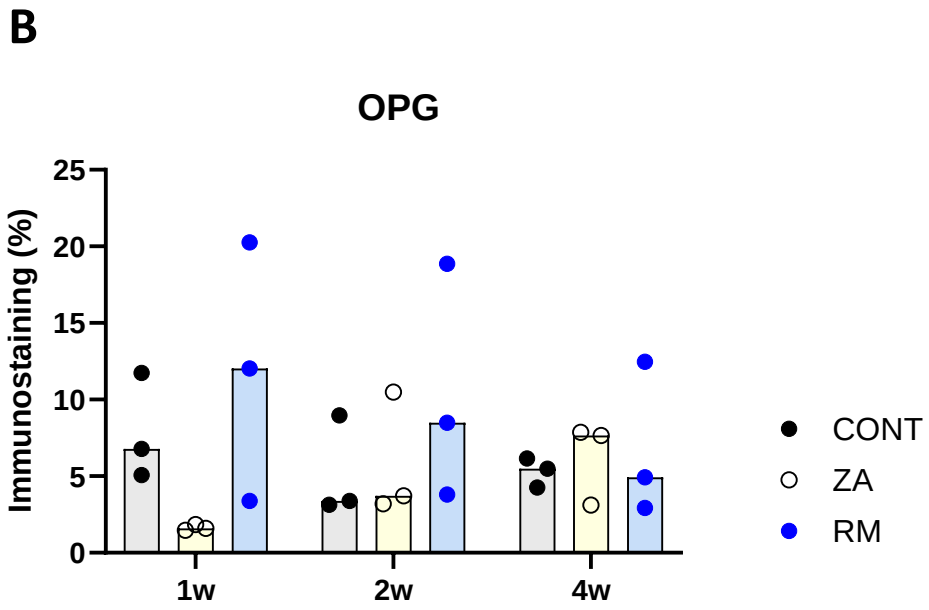

Figure 18. H-score of OPG on graft side : scatter plot, median with bar

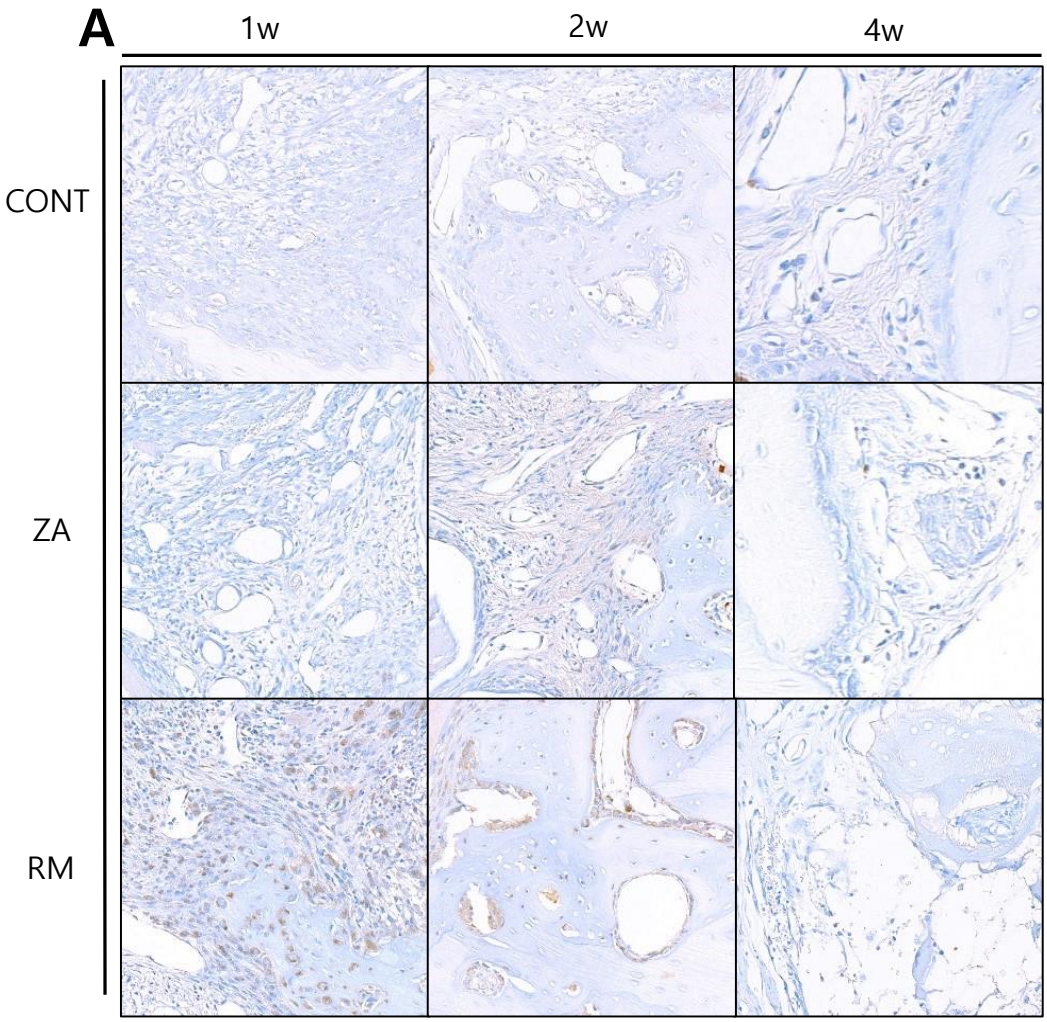

Figure 19. Immunohistochemical analysis of calvaria graft side : Sclerostin medial side image.

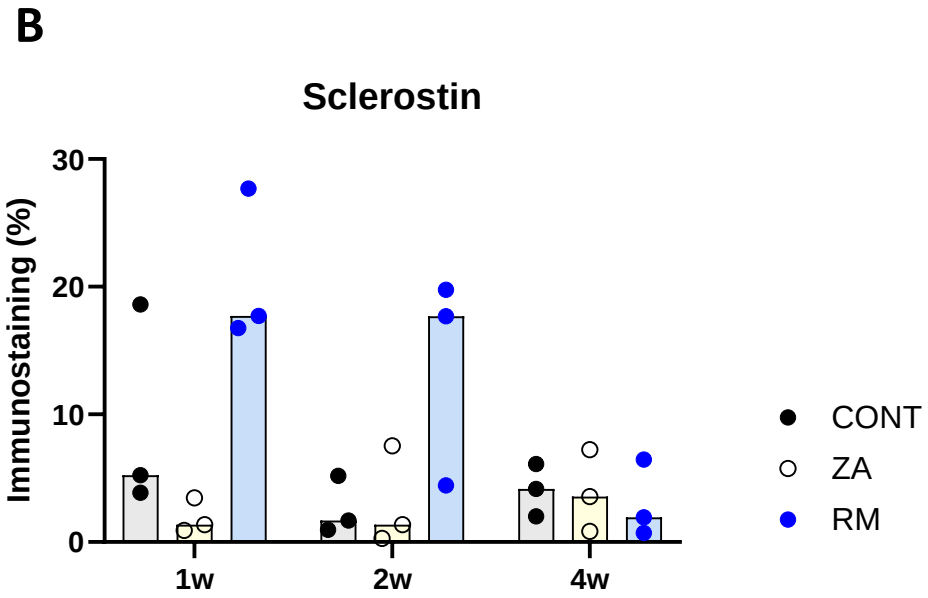

Figure 20. H-score of Sclerostin on graft side : scatter plot, median with bar.

The results from the H-score quantification of staining showed no statistical differences between time points or drugs. Regarding the staining intensity of sclerostin, the RM group exhibited higher sclerostin staining at the 1-week and 2-week time points compared to the CONT and ZA groups. However, at the 4-week time point, the staining intensity significantly decreased compared to the 1-week and 2-week time points. (Figure 15-20)

3.4. Calvaria bone : non graft side

3.4.1. Radiographic analysis : micro-computed tomography (micro-CT)

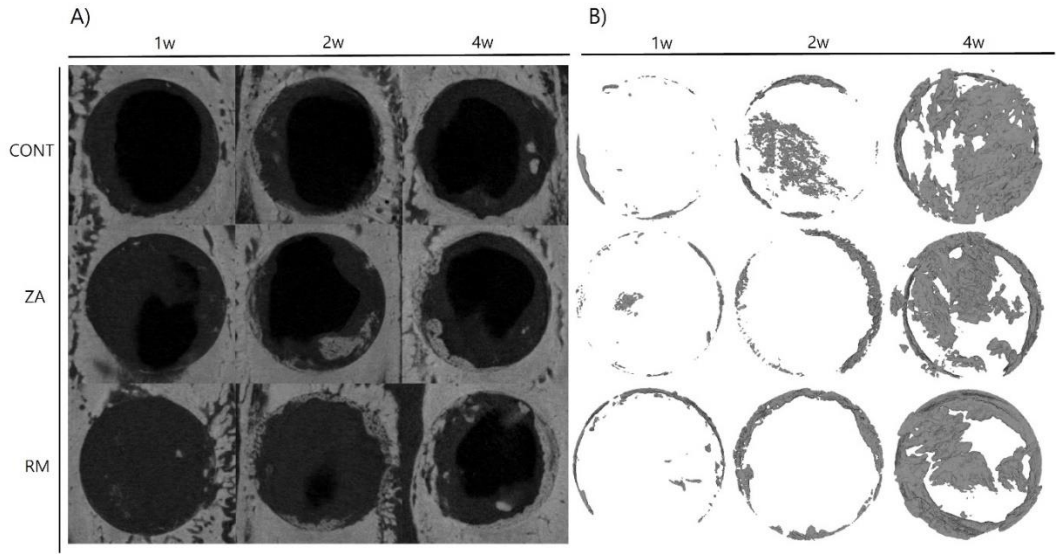

Figure 21. Micro-CT of calvaria bone : non-graft side (A) micro-CT image (B) 3D modeling of new bone of calvaria bone defect of non-graft side.

Figure 21(B) is 3D modeling of the new bone on the non-graft side of the calvaria bone. In the CONT, ZA, and RM groups, bone formation starts around the margin at 1 week, and as time progresses, bone is formed at the center of the defect and both above and below the defect. (Figure 21)

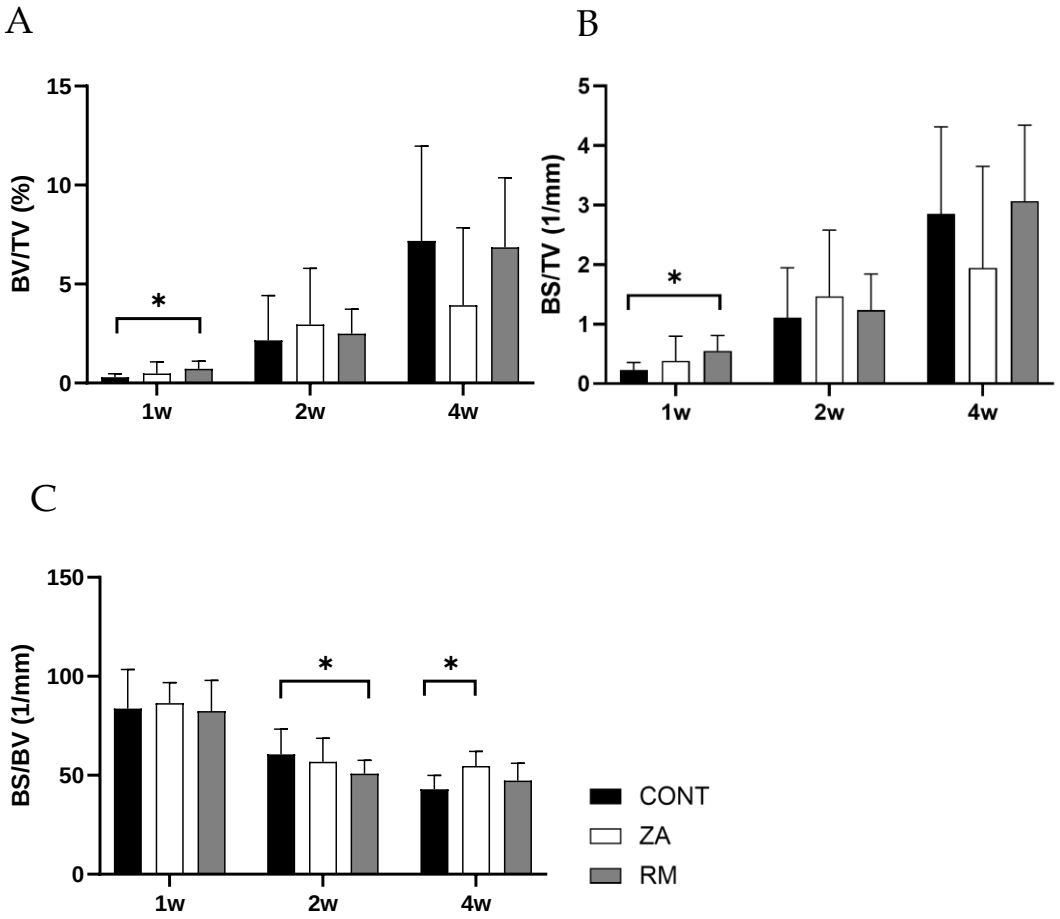

Figure 22. Micro-CT analysis of calvaria non-graft side : New bone (gray scale : 35-53) (A) Bone volume fraction (BV/TV, %), (B) Bone surface density (BS/TV,1/ mm), (C) Specific bone surface (BS/BV, 1/ mm). * indicate $p<0.017$.

As the drug administration period increased, both the bone volume fraction and bone surface density of new bone showed a similar trend of increase, with statistical differences observed only between CONT and RM at the 1-week time point. Specific bone surface showed a tendency to decrease as the drug administration period lengthened, with statistical differences between CONT and RM at 2 weeks, and between CONT and ZA at 4 weeks. (Figure 22)

3.4.2. Histological observation

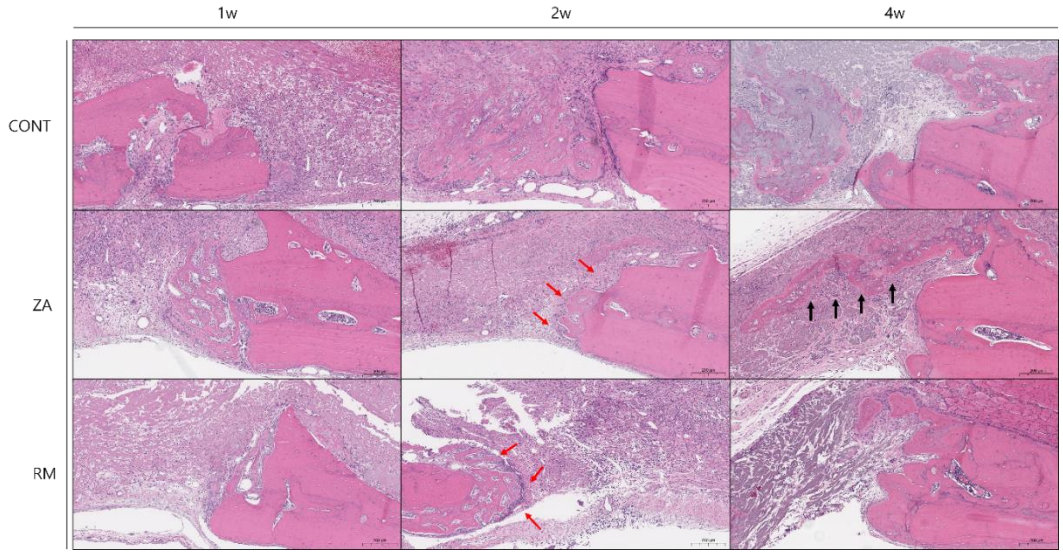

Figure 23. Histological findings in calvaria defect non-graft area H&E staining (100x).

In all groups, the defect was not completely closed. New bone formation was observed starting from the reversal line of the bone defect (red arrow), and new bone was also formed above the defect (black arrow). (Figure 23)

3.4.3. Histomorphometric analysis

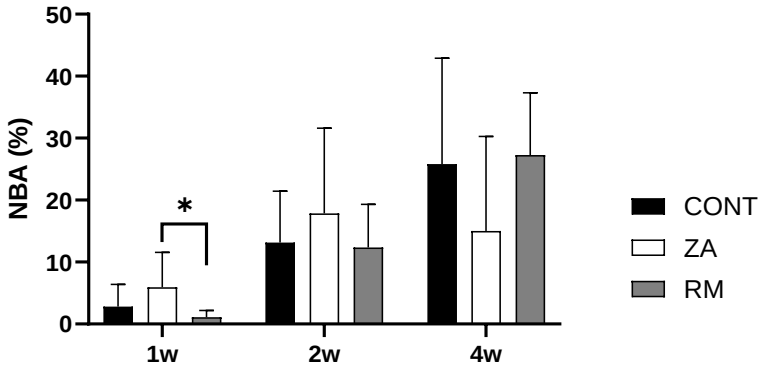

Figure 24. Histomorphometric analysis of calvaria non-graft side. * indicate $p<0.017$.

In the histological area analysis, as the drug administration period increased, more new bone formation was observed. In the 1-week treatment group, the areas of new bone in the RM and ZA groups showed a statistical difference. ZA showed the greatest new bone formation at 2 weeks, but it decreased by 4 weeks, while CONT and RM groups showed a continuous trend without a decrease. However, no statistical differences were observed at the 2-week and 4-week time points. (Figure 24)

3.4.4. Immunohistochemical (IHC) analysis

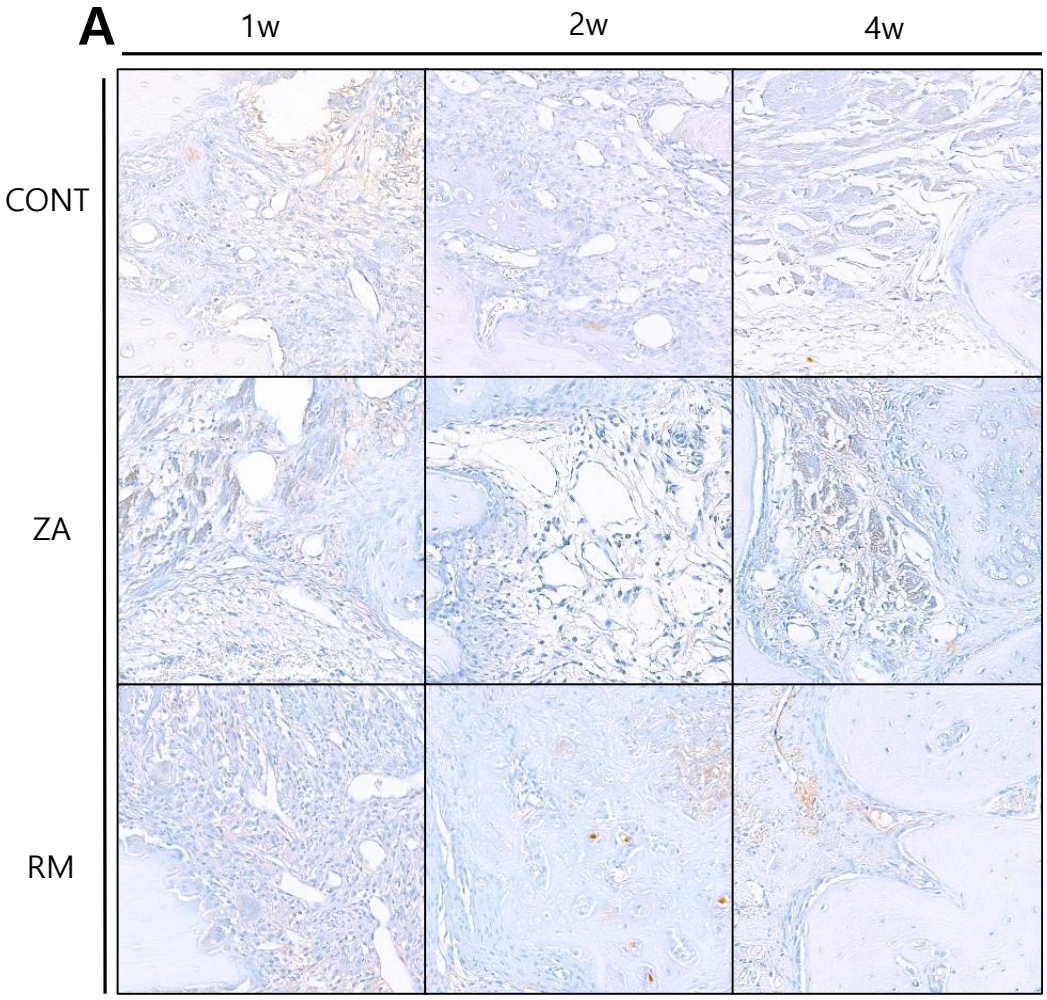

Figure 25. Immunohistochemical analysis of calvaria non graft side : RANKL medial side image

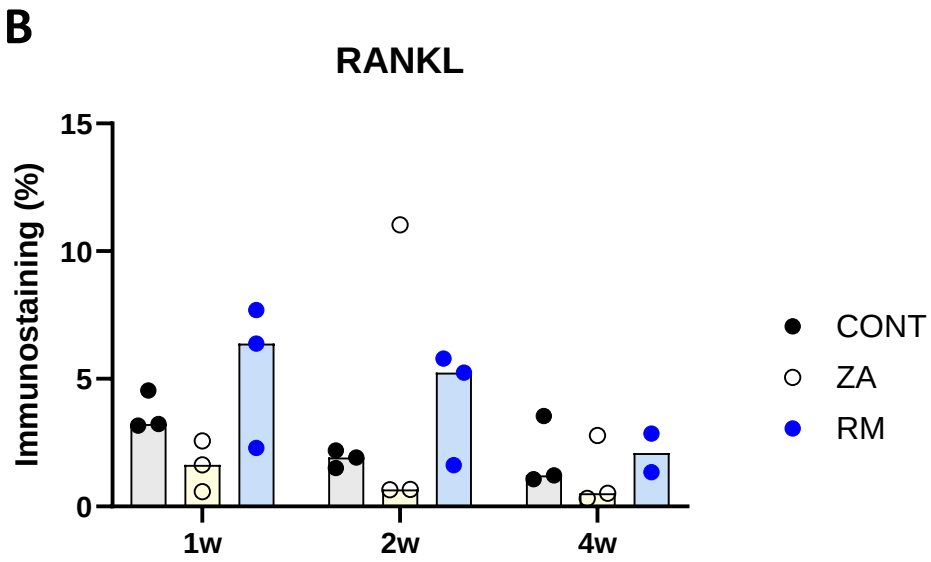

Figure 26. H-score of RANKL on non-graft side : scatter plot, median with bar

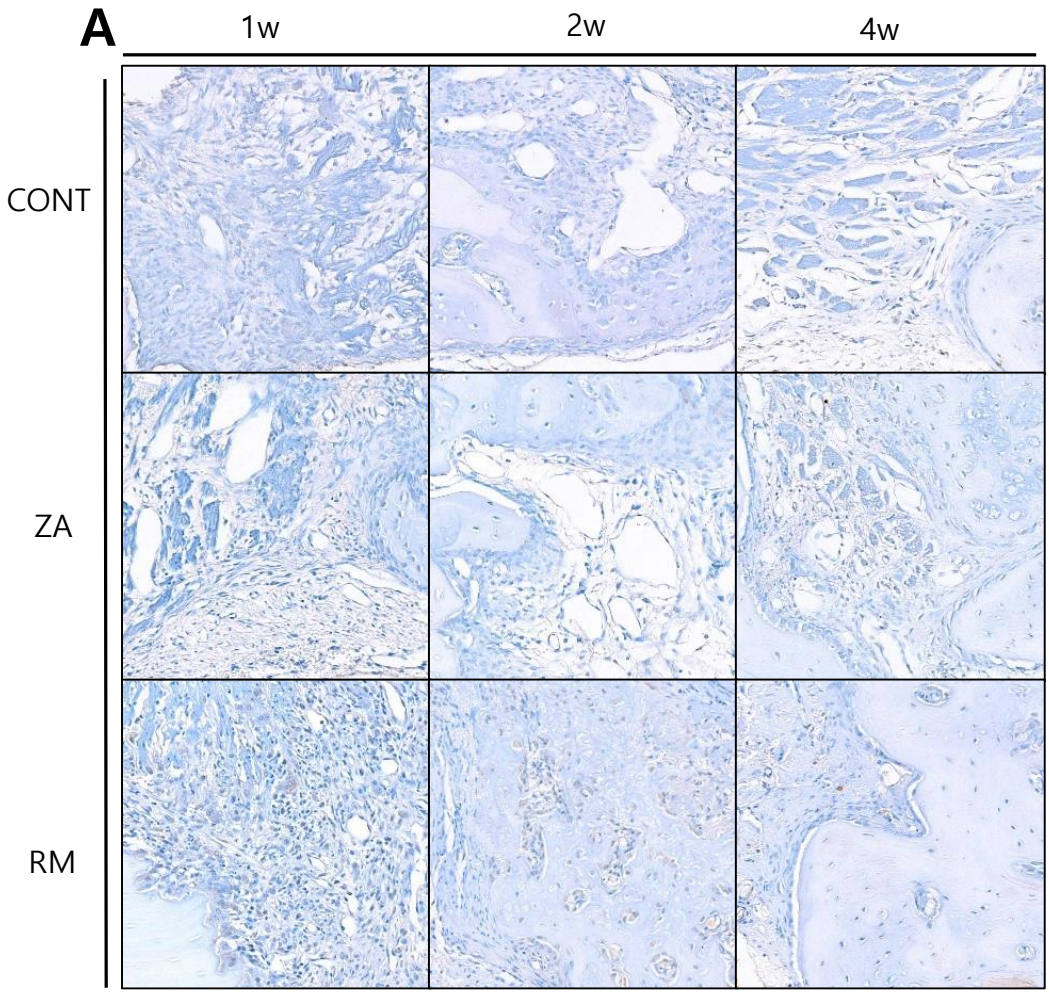

Figure 27. Immunohistochemical analysis of calvaria non-graft side : OPG medial side image

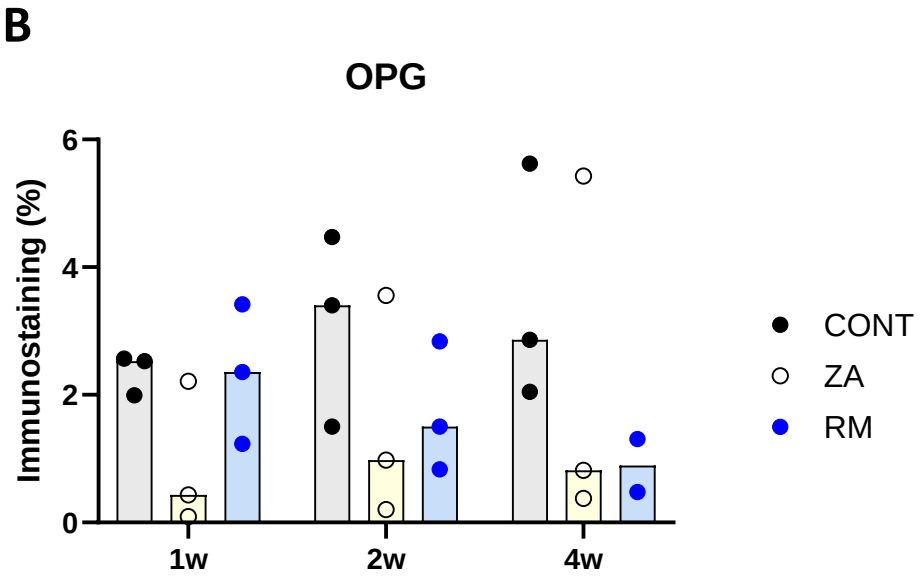

Figure 28. H-score of OPG on non-graft side : scatter plot, median with bar

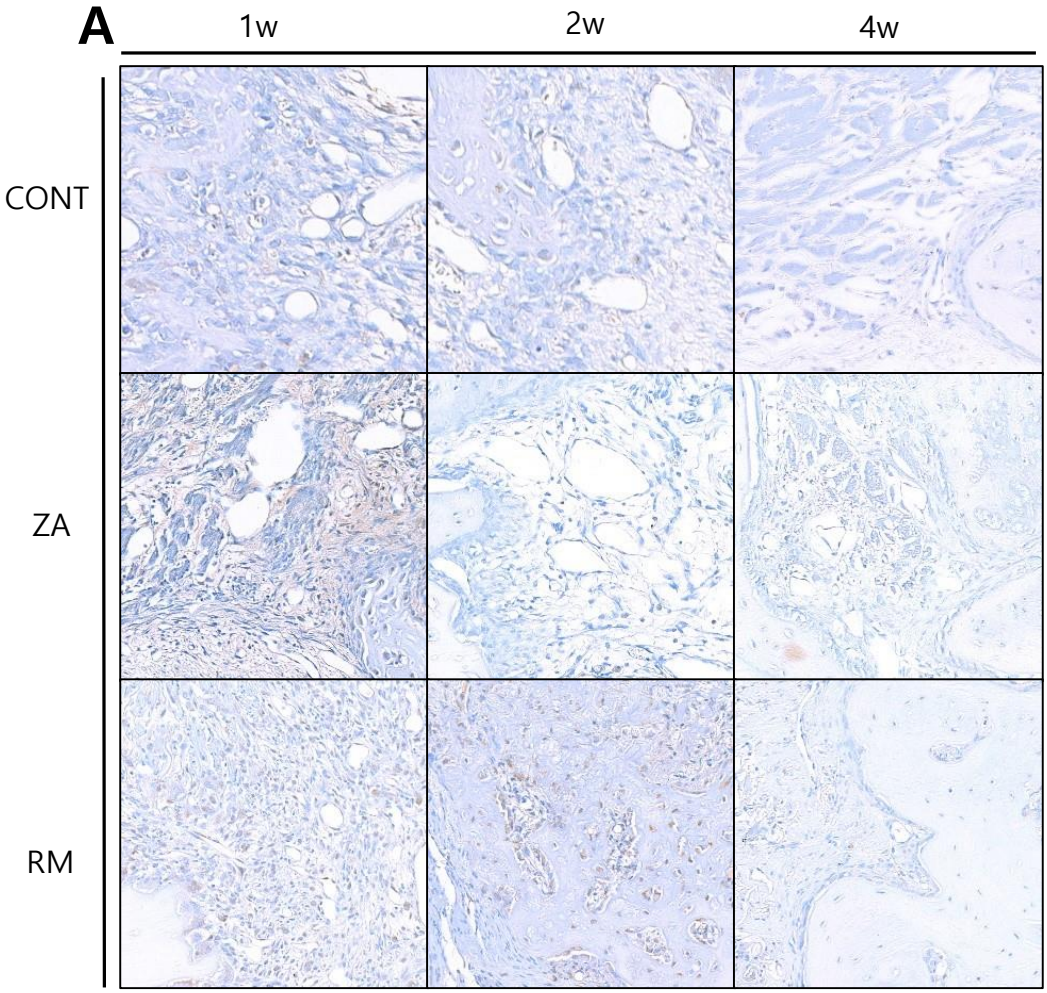

Figure 29. Immunohistochemical analysis of calvaria non-graft side : Sclerostin medial side image

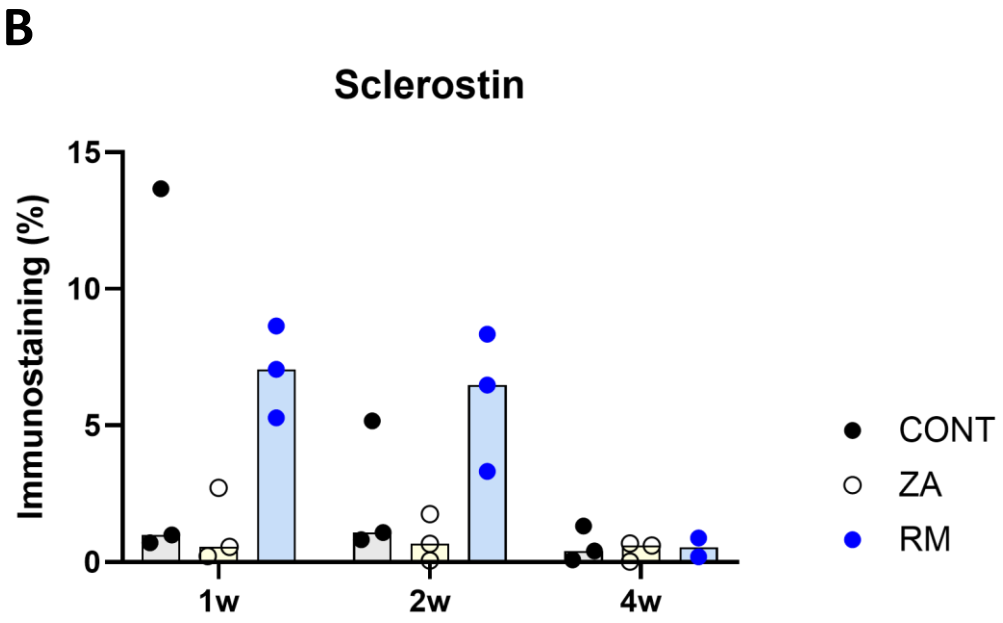

Figure 30. H-score of Sclerostin on non-graft side : scatter plot, median with bar

No statistical differences were observed between the groups for the staining intensity at each time point and for each drug, as quantified by H-score. The median values of RANKL, OPG, and Sclerostin showed a decreasing trend with the increase in drug administration period, but no statistical differences were found between the drug treatment groups. Regarding the staining intensity of sclerostin, in the RM group, the staining intensity was higher than that in the CONT and ZA groups at 1 and 2 weeks. However, at 4 weeks, the staining intensity decreased significantly compared to 1 and 2 weeks, showing a more pronounced reduction than in the CONT and ZA groups. (Figure 25-30)

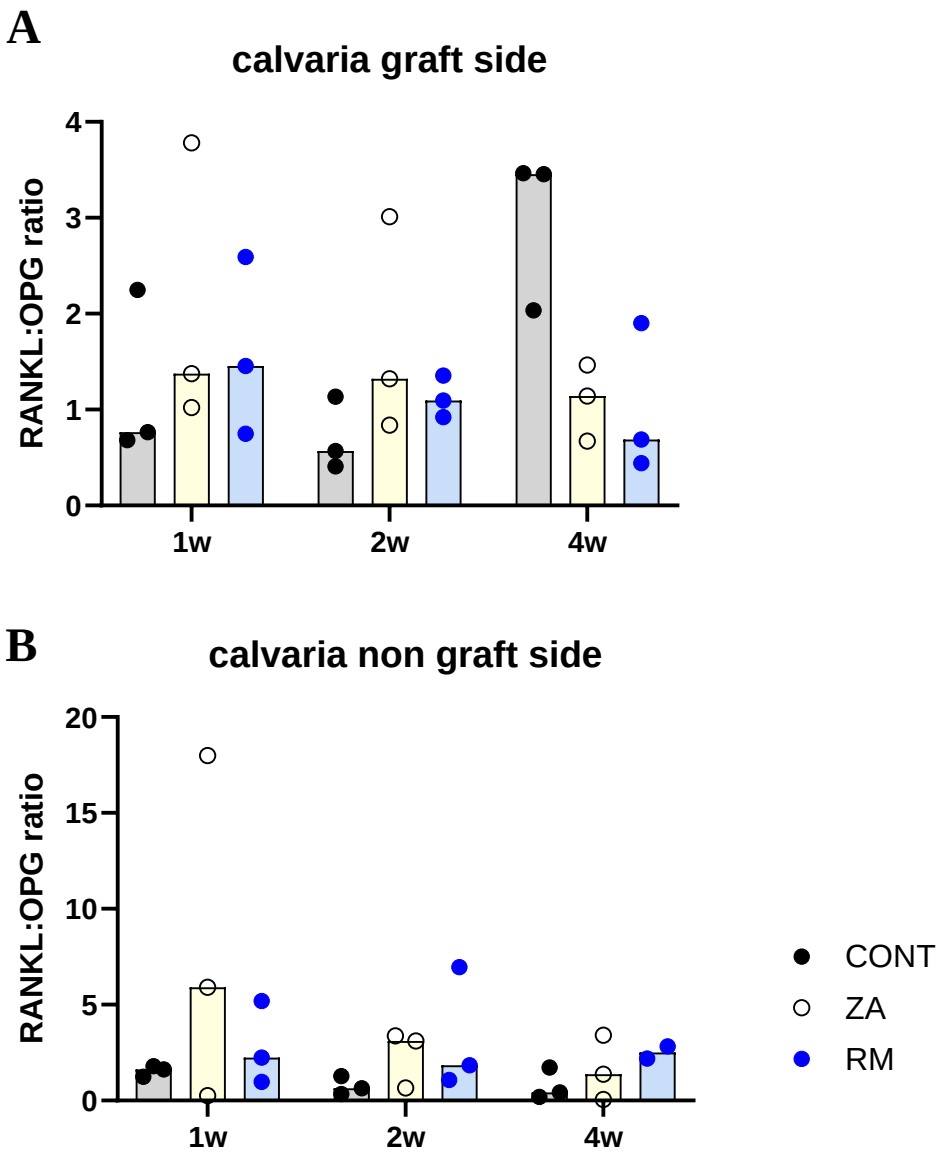

Figure 31. RANKL/OPG ratio. (A) calvaria graft side, (B) calvaria non graft side

In the calvaria graft side, the RANKL/OPG ratio in the ZA and RM groups gradually decreased with the length of drug administration, while the CONT group showed the highest value at 4 weeks. On the non-graft side, the RANKL/OPG ratio also showed a gradual decrease with the length of drug administration. No statistical significance was observed between the drug groups at any time point.(Figure 25)

4. Discussion

This study aimed to compare the effects of bone regeneration in calvaria defects when bone grafting was performed or not, under systemic administration of bisphosphonate and romosozumab in a rat model of experimentally induced osteoporosis. Clinically, this situation assumes bone grafting for oral reconstruction in osteoporosis patients with alveolar bone loss due to estrogen deficiency after menopause. While it is known that osteoporosis leads to a decrease in bone strength and an increased risk of fractures, little is known about bone regeneration and healing in osteoporosis patients (30). Additionally, there is a need for research on the effects of osteoporosis treatments on jaw bones, which may influence bone metabolism.

In this experiment, osteoporosis was induced in rats through ovariectomy to create estrogen deficiency, which is a commonly used animal model in postmenopausal osteoporosis research (31–33). Rodent models are frequently chosen for experiments not only in this study but also in many others due to their cost-effectiveness ratio, easier housing and handling, and the ability to standardize experimental conditions in genetically similar individuals (34).

In this experiment, to evaluate the systemic effects of osteoporosis drugs, changes in the microstructure of the tibia bone were observed. The results showed that after 4 weeks of drug administration, both ZA and RM groups had increased BV/TV compared to the CONT group, with RM showing a significant difference from CONT. Additionally, trabecular thickness was different in the 2-week and 4-week dosing groups, with differences observed between the CONT, ZA, and RM groups, which were also confirmed by histological staining. The effect of anabolic drugs like this is consistent with findings from a previous study using Cynomolgus monkeys, in which sclerostin antibody treatment resulted in a shift from rod-like trabeculae to plate-like trabeculae, thereby increasing trabecular thickness (35). Moreover, micro-CT of the zoledronic acid treatment

group showed an increased intensity in the growth plate. Previous studies have shown that RANKL and RANK deficient mice did not generate osteoclasts and exhibited thickened hypertrophic cartilage zones in their growth plates (36). Based on this, it can be confirmed that the drug inhibits osteoclast activity in the ZA group, affecting the tibia bone.

Regarding jaw bone regeneration in rats, bone regeneration was evaluated in critical size defects of the calvaria bone. In animal experiments, critical size defects in the calvaria are commonly used to evaluate bone healing. The critical size defect is defined as "the smallest size intra-osseous wound in a particular bone and species that will not heal spontaneously during the lifetime of the animal," a concept initially defined by Schmitz & Hollinger. However, due to experimental limitations, Gosain redefined it as "the critical-size defect in animal research refers to the size of a defect that will not heal over the duration of the study" (34,37,38). In this experiment, critical size defects with a diameter of 5 mm were created on both sides of the rat calvaria centered around the suture, and bone healing was evaluated based on the presence or absence of grafting. The study aims to assess how osteoporosis drugs, which affect bone metabolism, influence bone healing and regeneration.

According to the study by Durao et al. in 2012, when a calvaria critical bone defect was created in OVX rats, the formation of new bone was less compared to the sham group. In Durao et al.'s 2014 study, after creating a calvaria critical bone defect in OVX rats and evaluating biomaterial-mediated bone regeneration, histological and micro-CT analyses showed a quantitative decrease in the OVX group. Gene expression analysis also revealed a decrease in the expression of osteogenesis-related genes and changes in the expression of estrogen receptors and adipocyte markers in the regenerating bone of OVX animals (30,39). Similarly, in a study by Calciolari et al., when a bone graft was applied to a calvaria critical size defect in rats, OVX rats showed a decrease in new bone formation histologically after more than 30 days (40). This confirms that osteoporosis leads to a decreased

bone healing capacity in rat calvaria bone, and it is expected that bone regeneration will be reduced when bone grafts are performed in osteoporosis patients clinically.

In this experiment, the non-graft side was used to evaluate the healing of the critical size defect (CSD). Previous studies have shown conflicting results regarding the effect of Zoledronic acid on new bone formation in rat calvaria critical size defects after experimentally induced osteoporosis through OVX. Some studies report no significant difference (41), while others show an increase in new bone formation (42). In this experiment, both micro-CT and histological quantitative evaluations showed an increase in new bone formation as the drug administration period extended in the CONT, ZA, and RM groups. However, when comparing the drugs, a statistically significant difference was only observed in some assessments at week 1, and no consistent statistical significance was observed throughout the study. This could also be interpreted from the immunohistochemical staining results, where consistent statistical differences in RANKL, OPG, and sclerostin staining intensity were not observed.

RANKL/RANK signaling regulates the formation, activation, and survival of osteoclasts in normal bone modeling and remodeling, playing a crucial role in various pathological conditions where bone turnover is increased. OPG prevents excessive resorption by blocking the binding of RANKL to RANK, thus protecting the bone. Therefore, the relative concentrations of RANKL and OPG in the bone are key factors in determining bone mass and strength (36). RANKL promotes the survival, activation, and differentiation of osteoclasts, while Zoledronic acid reduces the expression of RANKL and increases the expression of OPG. Sclerostin antibody also indirectly inhibits the expression of RANKL and increases OPG expression, thereby reducing osteoclast activation (29,43).

In this study, the non-graft side showed a decrease in RANKL expression in the ZA group at all time points (1, 2, 4 weeks) compared to the CONT group, but an increase in the RM group. However, there was no statistical difference between the drug groups. For OPG, both the ZA and RM groups

showed a decrease compared to the CONT group. In the case of sclerostin, the RM group, which received the sclerostin antibody, showed higher staining intensity at 1 and 2 weeks, but by 4 weeks, the staining intensity decreased to levels similar to CONT and ZA groups. However, no statistically significant differences were observed even at week 4.

The graft side in this study was used to evaluate biomaterial-mediated bone regeneration by adding bone graft material to the critical size defect (CSD). Previous studies have shown conflicting results regarding Zoledronic acid in OVX-induced osteoporosis rats with respect to bone grafting in calvaria critical size defects. Some studies report no significant difference in new bone formation (41), while others report an increase in new bone formation (42). In this study, micro-CT analysis showed that, at week 4, the total bone volume fraction was significantly higher in the ZA group compared to the CONT group. Histological area calculations also showed increased new bone formation in the RM group compared to CONT at week 4. Immunohistochemical staining for RANKL showed a smaller value in the ZA group compared to CONT at all time points except for week 2, and the RM group also showed smaller values compared to CONT, but no statistical differences were observed. For OPG, the ZA group showed a significantly larger value at week 4 compared to CONT, and the RM group showed larger values compared to CONT at weeks 1 and 2. For sclerostin, the RM group showed higher values at weeks 1 and 2, similar to the non-graft side, but a lower value than CONT at week 4.

When considering the RANKL/OPG ratio on both the non-graft side and graft side, as well as various other indicators, it can be interpreted that, compared to the CONT group, the ZA and RM groups did not show consistent patterns in bone resorption, bone formation, and resolution according to their mechanisms of action. However, since indicators showing trends similar to the expected results were observed in the 4-week group, it is anticipated that a longer treatment period beyond 4 weeks would allow for a more consistent and clearer evaluation of the medication's effects.

Furthemore, despite the relatively clear structural changes observed in the tibia bone due to drug administration, no distinct differences are observed in the healing of the calvaria bone defect. Previous studies have also shown differences in healing speeds between tibia and calvaria defects in rats, which are explained by the differences in the periosteum between long bones and flat bones (44, 45).

In this experiment, groups that did not undergo ovariectomy (OVX) were not tested; however, previous studies on the calvaria critical size defect (CSD) model without OVX can serve as a substitute (30,40). However, there is a limitation in directly comparing the effects of the drugs in cases where osteoporosis has not occurred. To improve the experimental integrity, further experiments and studies on this aspect should be conducted in the future. The reason for setting the drug treatment periods at 1 and 2 weeks in this study is based on previous research that demonstrated the anabolic effect of sclerostin antibody on long bones in the early stages (20). If the effects of long-term drug administration are examined, it is believed that pharmacological actions could be observed more consistently.

5. Conclusion

In the ovariectomized rat menopause osteoporosis model, the RM group shows an increase in bone mass by thickening trabecular thickness in the tibia bone. However, in the calvaria critical size defect (CSD), no significant differences in bone regeneration were observed among the drugs, regardless of the presence of a graft

REFERENCES

1. Genant HK, Cooper C, Poor G, Reid I, Ehrlich G, Kanis J, et al. Interim report and recommendations of the World Health Organization Task-Force for Osteoporosis. Osteoporos Int J Establ Result Coop Eur Found Osteoporos Natl Osteoporos Found USA. 1999;10(4):259–64.

2. Singh S, Dutta S, Khasbage S, Kumar T, Sachin J, Sharma J, et al. A systematic review and meta-analysis of efficacy and safety of Romosozumab in postmenopausal osteoporosis. Osteoporos Int J Establ Result Coop Eur Found Osteoporos Natl Osteoporos Found USA. 2022 Jan;33(1):1–12.

3. Jeon Y, Kim IJ. Pharmacological treatment of osteoporosis: 2022 update. J Korean Med Assoc. 2022 Apr 10;65(4):241–8.

4. Reszka AA, Rodan GA. Nitrogen-containing bisphosphonate mechanism of action. Mini Rev Med Chem. 2004 Sep;4(7):711–9.

5. Bia M. Evaluation and management of bone disease and fractures post transplant. Transplant Rev Orlando Fla. 2008 Jan;22(1):52–61.

6. Hernlund E, Svedbom A, Ivergård M, Compston J, Cooper C, Stenmark J, et al. Osteoporosis in the European Union: medical management, epidemiology and economic burden: a report prepared in collaboration with the International Osteoporosis Foundation (IOF) and the European Federation of Pharmaceutical Industry Associations (EFPIA). Arch Osteoporos. 2013;8:1–115.

7. Hellstein JW, Adler RA, Edwards B, Jacobsen PL, Kalmar JR, Koka S, et al. Managing the care of patients receiving antiresorptive therapy for prevention and treatment of osteoporosis: executive summary of recommendations from the American Dental Association Council on Scientific Affairs. J Am Dent Assoc 1939. 2011 Nov;142(11):1243–51.

8. Reszka AA, Rodan GA. Bisphosphonate mechanism of action. Curr Rheumatol Rep. 2003 Feb;5(1):65-74.

9. Pavlakis N, Schmidt R, Stockler M. Bisphosphonates for breast cancer. Cochrane Database Syst Rev. 2005 Jul 20;(3):CD003474.

10. Reid IR, Brown JP, Burckhardt P, Horowitz Z, Richardson P, Trechsel U, et al. Intravenous zoledronic acid in postmenopausal women with low bone mineral density. N Engl J Med. 2002 Feb 28;346(9):653–61.

11. Lim SY, Bolster MB. Profile of romosozumab and its potential in the management of osteoporosis. Drug Des Devel Ther. 2017;11:1221–31.

12. Poole KES, van Bezooijen RL, Loveridge N, Hamersma H, Papapoulos SE, Löwik CW, et al. Sclerostin is a delayed secreted product of osteocytes that inhibits bone formation. FASEB J Off Publ Fed Am Soc Exp Biol. 2005 Nov;19(13):1842–4.

13. Cosman F, Crittenden DB, Adachi JD, Binkley N, Czerwinski E, Ferrari S, et al. Romosozumab Treatment in Postmenopausal Women with Osteoporosis. N Engl J Med. 2016 Oct 20;375(16):1532–43.

14. Aguirre JI, Castillo EJ, Kimmel DB. Preclinical models of medication-related osteonecrosis of the jaw (MRONJ). Bone. 2021 Dec;153:116184.

15. Jee JH, Lee W, Lee BD. The influence of alendronate on the healing of extraction sockets of ovariectomized rats assessed by in vivo micro-computed tomography. Oral Surg Oral Med Oral Pathol Oral Radiol Endod. 2010 Aug;110(2):e47-53.

16. Giro G, Gonçalves D, Sakakura CE, Pereira RMR, Marcantonio Júnior E, Orrico SRP. Influence of estrogen deficiency and its treatment with alendronate and estrogen on bone density around osseointegrated implants: radiographic study in female rats. Oral Surg Oral Med Oral Pathol Oral Radiol Endod. 2008 Feb;105(2):162–7.

17. Verzola MHA, Frizzera F, de Oliveira GJPL, Pereira RMR, Rodrigues-Filho UP, Nonaka KO, et al. Effects of the long-term administration of alendronate on the mechanical properties of the basal bone and on osseointegration. Clin Oral Implants Res. 2015 Dec;26(12):1466–75.

18. Frizzera F, Verzola MHA, de Molon RS, de Oliveira GJPL, Giro G, Spolidorio LC, et al. Evaluation of bone turnover after bisphosphonate withdrawal and its influence on implant osseointegration: an in vivo study in rats. Clin Oral Investig. 2019 Apr;23(4):1733–44.

19. Suen PK, He YX, Chow DHK, Huang L, Li C, Ke HZ, et al. Sclerostin monoclonal antibody enhanced bone fracture healing in an open osteotomy model in rats. J Orthop Res Off Publ Orthop Res Soc. 2014 Aug;32(8):997–1005.

20. Ominsky MS, Boyce RW, Li X, Ke HZ. Effects of sclerostin antibodies in animal models of osteoporosis. Bone. 2017 Mar;96:63–75.

21. Hosseinpour S, Rad MR, Khojasteh A, Zadeh HH. Antibody Administration for Bone Tissue Engineering: A Systematic Review. Curr Stem Cell Res Ther. 2018;13(4):292–315.

22. Yu SH, Hao J, Fretwurst T, Liu M, Kostenuik P, Giannobile WV, et al. Sclerostin-Neutralizing Antibody Enhances Bone Regeneration Around Oral Implants. Tissue Eng Part A. 2018 Nov;24(21–22):1672–9.

23. Taut AD, Jin Q, Chung JH, Galindo-Moreno P, Yi ES, Sugai JV, et al. Sclerostin antibody stimulates bone regeneration after experimental periodontitis. J Bone Miner Res Off J Am Soc Bone Miner Res. 2013 Nov;28(11):2347–56.

24. Chen H, Xu X, Liu M, Zhang W, Ke H zhu, Qin A, et al. Sclerostin antibody treatment causes greater alveolar crest height and bone mass in an ovariectomized rat model of localized periodontitis. Bone. 2015 Jul;76:141–8.

25. Retzepi M, Donos N. Guided Bone Regeneration: biological principle and therapeutic applications. Clin Oral Implants Res. 2010 Jun;21(6):567–76.

26. Bouxsein ML, Boyd SK, Christiansen BA, Guldberg RE, Jepsen KJ, Müller R. Guidelines for assessment of bone microstructure in rodents using micro-computed tomography. J Bone Miner Res Off J Am Soc Bone Miner Res. 2010 Jul;25(7):1468–86.

27. Ahn H, Park W, Choi SH, Hong N, Huh J, Jung S. Effect of anti-sclerostin antibody on orthodontic tooth movement in ovariectomized rats. Prog Orthod. 2024 Nov 25;25(1):45.

28. Belluci MM, de Molon RS, Rossa C, Tetradis S, Giro G, Cerri PS, et al. Severe magnesium deficiency compromises systemic bone mineral density and aggravates inflammatory bone resorption. J Nutr Biochem. 2020 Mar;77:108301.

29. de Molon RS, Fiori LC, Verzola MHA, Belluci MM, de Souza Faloni AP, Pereira RMR, et al. Long-term evaluation of alendronate treatment on the healing of calvaria bone defects in rats. Biochemical, histological and immunohistochemical analyses. Arch Oral Biol. 2020 Sep;117:104779.

30. Durão SFO, Gomes PS, Silva-Marques JM, Fonseca HRM, Carvalho JFC, Duarte JAR, et al. Bone regeneration in osteoporotic conditions: healing of subcritical-size calvaria defects in the ovariectomized rat. Int J Oral Maxillofac Implants. 2012;27(6):1400–8.

31. Turner AS. Animal models of osteoporosis--necessity and limitations. Eur Cell Mater. 2001 Jun 22;1:66–81.

32. Turner RT, Maran A, Lotinun S, Hefferan T, Evans GL, Zhang M, et al. Animal models for osteoporosis. Rev Endocr Metab Disord. 2001 Jan;2(1):117–27.

33. Komori T. Animal models for osteoporosis. Eur J Pharmacol. 2015 Jul 15;759:287–94.

34. Vajgel A, Mardas N, Farias BC, Petrie A, Cimões R, Donos N. A systematic review on the critical size defect model. Clin Oral Implants Res. 2014 Aug;25(8):879–93.

35. Matheny JB, Torres AM, Ominsky MS, Hernandez CJ. Romosozumab Treatment Converts Trabecular Rods into Trabecular Plates in Male Cynomolgus Monkeys. Calcif Tissue Int. 2017 Jul;101(1):82–91.

36. Boyce BF, Xing L. Functions of RANKL/RANK/OPG in bone modeling and remodeling. Arch Biochem Biophys. 2008 May 15;473(2):139–46.

37. Schmitz JP, Hollinger JO. The critical size defect as an experimental model for craniomandibulofacial nonunions. Clin Orthop. 1986 Apr;(205):299–308.

38. Gosain AK, Song L, Yu P, Mehrara BJ, Maeda CY, Gold LI, et al. Osteogenesis in cranial defects: reassessment of the concept of critical size and the expression of TGF-beta isoforms. Plast Reconstr Surg. 2000 Aug;106(2):360–71; discussion 372.

39. Durão SF, Gomes PS, Colaço BJ, Silva JC, Fonseca HM, Duarte JR, et al. The biomaterial-mediated healing of critical size bone defects in the ovariectomized rat. Osteoporos Int J Establ Result Coop Eur Found Osteoporos Natl Osteoporos Found USA. 2014 May;25(5):1535–45.

40. Calciolari E, Mardas N, Dereka X, Kostomitsopoulos N, Petrie A, Donos N. The effect of experimental osteoporosis on bone regeneration: Part 1, histology findings. Clin Oral Implants Res. 2017 Sep;28(9):e101–10.

47. Park KM, Lim GY. Bone Regeneration Assessment after Systemic Injection of Bisphosphonate and Parathyroid Hormone in the Ovariectomized Rat. Calvaria Defect J Korean Academy of Advanced General Dentistry. 2023;12:97-106

42. Mardas N, Busetti J, de Figueiredo JAP, Mezzomo LA, Scarparo RK, Donos N. Guided bone regeneration in osteoporotic conditions following treatment with zoledronic acid. Clin Oral Implants Res. 2017 Mar;28(3):362–71.

43. Marini F, Giusti F, Palmini G, Brandi ML. Role of Wnt signaling and sclerostin in bone and as therapeutic targets in skeletal disorders. Osteoporos Int J Establ Result Coop Eur Found Osteoporos Natl Osteoporos Found USA. 2023 Feb;34(2):213–38.

44. Lim J, Lee J, Yun HS, Shin HI, Park EK. Comparison of bone regeneration rate in flat and long bone defects: Calvaria and tibial bone. Tissue Eng Regen Med. 2013 Dec 1;10(6):336–40.

45. Fujii T, Ueno T, Kagawa T, Sakata Y, Sugahara T. Comparison of bone formation ingrafted periosteum harvested from tibia and calvaria. Microsc Res Tech. 2006 Jul;69(7):580–4.

Abstract in Korean

골다공증 유도된 백서의 졸레드론산과 로모소주맙에 대한 두개골 결손부 골재생 비교

<지도교수 박원서>

연세대학교 대학원 치의학과

이경진

본 실험은 난소절제술을 받은 백서 골다공증 모델에서 졸레드론산과 로모소주맙을 투여하였을 때 두개골 임계결손의 골재생에 대한 두 약물의 영향을 평가하고자 하는 것이다. 이는 골다공증 약물을 투약중인 환자에게 임플란트 식립이나 치조골 골결손부위에 골이식를 시행한 경우에 골대사에 영향을 주는 골다공증 약물의 효과를 동물실험 모델을 통해 확인하고자 하는 연구이다.

난소절제술을 받은 백서를 약물의 종류와 약물 투약기간에 따라 9 개의 그룹으로 나누었다. : control(CONT) 1w group, control(CONT) 2w group, control(CONT) 4w group, zoledronic acid (ZA) 1w group, zoledronic acid (ZA) 2w group, zoledronic acid (ZA) 4w group, romosozumab (RM) 1w group, romosozumab(RM) 2w group, romosozumab(RM) 4w group. CONT group 에는 아무런 약물을 투약하지 않았고, ZA group 과 RM group 은 1 주, 2 주, 4 주 동안 각각 졸레드론산과 로모소주맙을 투약하였다. 모든 실험 개체의 두개골에 5mm 의 원형의 결손을

양측으로 형성하였고, 한쪽에는 골이식을 시행, 다른 한쪽은 골이식을 시행하지 않았다. 약물의 전신적인 효과를 확인하기 위하여 경골에 대하여 방사선학적, 조직학적 검사를 시행하였고, 골재생의 효과를 확인을 위하여 두개골 결손부에 대하여 방사선학적, 조직학적, 면역조직화학 분석을 수행하였다.

경골에서는 RM 2 주, 4 주 투약그룹에서는 해면골의 두께가 증가하면서 뼈의 부피를 증가시킨다. 두개골의 골이식부에서는 조직학적 면적 계산에서 4 주 투약 RM group 이 CONT 에 비하여 통계적 차이를 보이며 신생골이 더 많이 형성된 것으로 보이나 조직면역화학 검사시에는 RANKL, OPG, sclerostin 에서의 통계적인 차이는 보이지 않는다. 골이식을 하지 않은 부위에도 방사선학적, 조직면역화학적 검사 시 약물 투약그룹과 CONT 차이에의 영향이 뚜렷하게 보이지 않는다.

경골에서의 골다공증 약물의 효과를 보았을 때, 로모소주맙이 졸레드론산에 비하여 해면골의 두께를 증가시키며 뼈의 부피를 증가시키는 양상을 보이나, 두개골 결손부에서는 골이식 유무에 관계없이 졸레드론산과 로모소주맙의 골재생에의 영향에 있어서는 차이를 보이지 않았다. 이는 경골과 두개골의 해부학적, 발생학적 차이에 기인하는 것으로 사료되며, 약물 투약 초기에의 영향에 있어서 경골과 두개골의 반응의 차이가 있는 것으로 예상된다. 향후 약물을 장기적으로 투약하였을 때의 영향에 대한 연구가 필요할 것으로 사료되며, 이는 골다공증 약물의 악골의 골재생에의 영향에 대한 기초 연구로서 가치를 가질 것으로 사료된다.

핵심되는 말: 졸레드론산, 로모소주맙, 골다공증, 임계결손, 골재생